A modelling-based assessment of suspended sediment transport related to new damming in the Red River basin from 2000 to 2013

Xi Wei, Sabine Sauvage, Sylvain Ouillon, Thi Phuong Quynh Le, Didier Orange, Marine Herrmann, J.M. Sánchez-Pérez

A modelling-based assessment of suspended sediment transport related to new damming in the Red River basin from 2000-2013

Xi Wei[1*], Sabine Sauvage[1**], Sylvain Ouillon[2,3], Thi Phuong Quynh Le[4], Didier Orange[5], Marine Herrmann[2,3], José-Miguel Sanchez-Perez[1]

[1]ECOLAB, Université de Toulouse, CNRS, INPT, UPS, Auzeville-Tolosane, France.

[2]LEGOS, Université de Toulouse, IRD, CNRS, UPS, Toulouse, France.

[3]USTH, Vietnam Academy of Science and Technology (VAST), Hanoi, Vietnam.

[4]Institute of Natural Product Chemistry (INPC), Vietnam Academy of Science and Technology (VAST), Hanoi, Vietnam.

[5]Eco & Sols, Univ. Montpellier, IRD, CIRAD, INRA, Montpellier SupAgro, Montpellier, France.

Correspondence

*Xi Wei, ECOLAB, Université de Toulouse, CNRS, INPT, UPS, Avenue de l'Agrobiopole, 31326 Auzeville-Tolosane, France.

Email: xi.wei_fr@hotmail.com

**Sabine Sauvage, ECOLAB, Université de Toulouse, CNRS, INPT, UPS, Avenue de l'Agrobiopole, 31326 Auzeville-Tolosane, France.

Email: sabine.sauvage@univ-tlse3.fr

Abstract:

The Red River is an Asian river system strongly affected by global changes. This paper aims to characterize and quantify the suspended sediment flux (SF) over the basin under the influences of short-term climate variability and dam constructions. SF was evaluated at the outlets of main tributaries and along the main course of the Red River from 2000 to 2013 based on daily simulations from a modelling study. A reference scenario (without dams) was carried out to disentangle the impacts of short-term climate variability and damming by comparing to actual conditions. Without dams (reference scenario), the basin would generate 106.9 Mt yr^{-1} of SF to the downstream delta from 2000 to 2013, with a specific sediment yield (SSY) of 778.8 t km^{-2} yr^{-1}. However, under the impacts of short-term climate variability and dams, the mean annual SSY decreased to 84.5 t km^{-2} yr^{-1}. At the outlet of the basin, the annual mean SF of 2008-2013 (after new dam constructions) got reduced by 90% (10% related to short-term climate or atmospheric variability and 80% to dam constructions) compared to the reference scenario (without dams) during 2000-2007. The Thao tributary is the most sensitive to short-term climate variability while the Da tributary is mostly affected by the huge-capacity dams. Mean annual retentions of sediment by dams ranged from 7.1 to 111.0 Mt yr^{-1}. Simple rating curves between monthly mean discharge (Q) and SF were established for estimating SF at the outlet of the tributaries and the Red River. High soil erosion (above 2000 t km^{-2} yr^{-1}) occurred in the middle Thao and the lower Da

tributaries. Precipitation, slope and agriculture practices are the key influence factors for soil erosion in the basin.

Keywords: suspended sediment, modelling, the Red River, short-term climate variability, dam, soil erosion.

1. INTRODUCTION

The suspended sediment (SS) transport from continents to oceans by rivers is a crucial process of sediment cycle in the Earth systems: this process drives associated elements to the seas, which is essential for marine biogeochemical cycle and diversity; also, it is a reflection of land and river degradation; besides, this process is of great importance in geomorphology, such as downstream delta formation (Dai et al., 2009; Kunz et al., 2011; Lal et al., 1995). Rivers contribute to 95% of the sediment fluxes (SF) to the oceans (Syvitski et al., 2003), which ranged from 15 to 20 billion t yr^{-1} (Beusen et al., 2015; Ludwig and Probst, 1996; Milliman and Meade, 1983; Ouillon, 2018; Vörösmarty et al., 2003). In particular, Asian rivers such as the Yellow River and the Mekong River contribute to a large part of sediment delivery to the seas (Cohen et al., 2014; Dang et al., 2018). However, climate variability and anthropogenic activities have altered the SF (Dai et al., 2009; Dang et al., 2018; Jiang et al., 2009).

Under anthropogenic disturbances such as intensive agriculture and damming, water ecosystems are facing severe challenges, like the increase of soil erosion, and changes of hydrology regime and SF (Chen et al., 2016; FAO, 2011a; IPCC, 2019; Valentin et al., 2008; Zimmerman et al., 2008). Dam construction is the factor with the strongest influence on land-ocean SF (Walling and Fang, 2003). According to the World Commission on Dams (2000), at least 45,000 large dams have been built globally, and nearly half of the world's rivers have one large dam at least. Lehner et al., (2011) found that around 28% of dams are located in Asia. Besides, future hydropower development is primarily concentrated in developing countries and emerging economies of Southeast Asia (Zarfl et al., 2015). Dams cause a significant reduction in SF. Vörösmarty et al. (2003) estimated that the potential sediment trapping by dams in regulated basins was higher than 50%. In some basins, such as the Colorado, Nile and Yellow rivers, sediment is completely trapped due to the large size of reservoirs and to the flow velocity decreases which weakens the sediment transportability (Peng et al., 2010; Vörösmarty et al., 2003; Walling and Fang, 2003). Reduced sediment transport can induce river deltas sinking, therefore affecting estuarine and coastal human communities (Hauer et al., 2018; Syvitski et al., 2005), and increasing their vulnerability (Lehner et al., 2011). Asian rivers constitute good indicators of the strong influence of anthropogenic activities on sediment transport (Arias et al., 2014; Dang et al., 2010; Furuichi et al., 2009).

The Red River is a typical Asian river system under the influences of global changes and is the second largest river in Vietnam. It gathers numerous inter-linked rivers, estuaries and coastal waters and plays an important role in agriculture and economy in this basin, which is a major agricultural production region. Understanding and quantifying the water and soil processes and budgets of this river basin will help to manage soil loads and also to study other Asian rivers. Hence, the objective of this paper is to assess the SS regime in a large Asian basin under the influences of global changes, especially under the impacts of dams. Moreover, it would be more precise to calculate SF at a daily time step as discharge (Q) and suspended sediment concentration (SSC) can vary greatly from day to day. However, few studies analyzed fluxes at daily scale in the Red River basin, focusing either on a short period (Le et al., 2007), or only on the outlet of the continental basin (Dang et al., 2010) or on the delta (Luu et al., 2010), or only on Q or SS (Hiep et al., 2018). Assessing SS regime at a daily time step at different stations in the Red River basin will, therefore, contribute to improving our knowledge of the SF across the whole basin.

For achieving this objective, a modelling approach, combining remote sensing and in-situ data, was used. The modelling setup and calibration were described in Wei et al. (2019). The specific objective of the present paper is: 1) to quantify SF of the Red River basin based on daily Q and SSC; 2) to disentangle and quantify the impacts of damming and short-term climate or atmospheric variability on SF; 3) to provide rating curves for estimating the SF at the outlets of the main tributaries and of the continental basin; 4) to identify the hot spots of soil erosion.

2. MATERIALS AND METHODS

2.1. Study area

The study area focuses on the Red River continental basin with a surface of

137,200 km^2 which drains down to Son Tay, the outlet of the continental basin and the entrance of the delta (Figure 1).

2.1.1. General characteristics

The Red River basin is located in Southeast Asia (Figure 1a), shared by China (49%), while Vietnam (50.1%) and Laos (0.9%).

Son Tay is a confluence of three main tributaries: the Lo River (named Panlong Jiang in China) on the left bank, the Thao River (named Yuan Jiang in China) upstream of the main river, and the Da River (named Lixian Jiang in China) on the right bank. They join the Red River 20 km upstream to the Son Tay gauging station.

The elevation ranges from 2650 m a.s.l. to 6 m a.s.l. in this basin (Wei et al., 2019). The upstream part of Lao Cai is mainly formed by tectonically active mountainous areas, with steep slopes, usually above 25° (Zhang et al., 2017) which are vulnerable to soil erosion due to the intensive precipitation and land use changes (Bai et al., 2015; Barton et al., 2004; He et al., 2007). The soil types are mainly Acrisols, such as red earth and yellow-brown soil (Bai et al., 2015; Le, 2005). High erosion plus the character of soil types color the water of the Thao River into “red” (Le, 2005). In Vietnam, the same Acrisols dominate on the slopes while grey or alluvial soils dominate in the valleys (Le et al., 2017).

In China’s part, the main land cover is forest (62%), followed by grassland (19%) and cultivated land (18%), respectively (Li et al., 2016a). In Vietnam’s part, in the Thao basin, forest is dominating, accounting for 54.2%, followed by rice paddy fields (19%) and industrial crops (13%); the Lo and Da basins are dominated by industrial crops (58%) and forests (74%), respectively (Le et al., 2007).

Figure 1. (a) The geographical location of the Red River basin in Southeast Asia; (b) locations of the dams (red triangle) and the hydrological gauge stations (blue point) in the Red River basin.Base maps sources were obtained from ArcGIS desktop.

2.1.2. Meteorological characteristics

The whole Red River basin encompasses two different climate zones: humid subtropical climate in the upper part and humid tropical climate in the lower part, and a strong seasonal variability related to the Southeast Asia monsoon system, which alternates between the cold and dry southwestward winter monsoon from November to April and the hot and humid northeastward summer monsoon from May to October. Rainfall during flood seasons (May to October) contributes to 85-90% of the whole year average (Le et al., 2007; Li et al., 2016b). The general trend of regional precipitation distribution increases from upstream (1000 to 1600 mm yr^{-1} in China) to downstream (1328 to 2255 mm yr^{-1} in Vietnam) (Le et al., 2007; Li et al., 2008; Xie, 2002). During 2000-2013, the mean annual rainfall through the Red River basin was 1494 mm yr^{-1} (Wei et al., 2019).

Temperature variations follow a typical orographic pattern, increasing with the decreasing of the elevations, from the northwest (mountainous regions) to the southeast. The mean annual temperature varies from 15 to 21 °C in China (Xie, 2002) and 14 to 27 °C in Vietnam (Le, 2005). During the year, the winter temperature ranges from 14-16 °C in winter and 27-29 °C in summer (Le, 2005; Lu et al., 2015).

2.1.3. Hydrological characteristics

Runoff is mainly recharged by precipitation which leads to big seasonal variations in river flows (FAO, 2011b; Li et al., 2016a; Li et al., 2008). The mean annual discharge during 2000-2013 at Son Tay was 3082 $m^3\ s^{-1}$ (Wei et al., 2019). Corresponding to the distribution of rainfall, the runoff is also unevenly distributed. More than 80% of the total annual runoff is produced during rainy seasons (May to October); runoff peaks usually occur in August, and the maximum flood reached 8050 $m^3\ s^{-1}$ in 1986 near the border in China (Xie, 2002), and 37,800 $m^3\ s^{-1}$ at Son Tay in 1971 (Luu et al., 2010). November to April is the dry season, and the minimum discharge occurs in March. The minimum discharge observed near the boundary in China was 28.7 $m^3\ s^{-1}$ in 1963 (Ren et al., 2007), and the minimum daily discharge at Son Tay during 2000-2013 was 493 $m^3\ s^{-1}$ (Wei et al., 2019).

2.1.4. Dams implementation

In recent years, to meet the water demand according to the rapid increase of population and intensive agriculture activities, dams have been constructed both in China and Vietnam. It is difficult to obtain all the information of all the dams located in the Thao and Lo rivers as most of their information is not accessible to the public, therefore, in this study, we only specifically took into account the dams with big capacity (>2.2 km^3) and located on the downstream part, i.e. close to the outlets of each tributary.

On the Thao River, twelve cascade reservoirs were built or are under construction in China's territory. The impoundment of the first two dams, the Nansha and the Madushan dams, located around 150 km and 100 km upstream of Lao Cai gauge station respectively, started on November 2007 and December 2010, respectively, and they are the only two dams impounded on the Thao River during the study period.

On the Da River, the biggest dam in Vietnam named Hoa Binh was put into use in 1989. A mass of solid materials has been trapped by this dam, which consequently reduces the dam's efficient capacity and lifetime (Dang et al., 2010). To mitigate the siltation of the Hoa Binh dam and to meet the need for economic growth, the Son La dam was built and put into operation in January 2011.

On the Lo River, the Thac Ba dam was implemented in 1972 and the Tuyen Quang dam in March 2008 (Table 1 and Figure 1).

Table 1 Basic characteristics of the main dams in the Red River basin (Le et al., 2017; Wei et al., 2019)

2.2. Data collection

Observed data of daily Q and SSC from 2000 to 2013 was obtained from the Vietnam Ministry of Natural Resources and Environment (MONRE) at Lao Cai, Yen Bai, Vu Quang, Hoa Binh and Son Tay gauge stations (Figure 1). Daily SS sampling campaigns were conducted at different gauge stations. SS was collected vertically from the water surface to the bottom by a collector at each station. Then in the laboratory, a known volume of well-mixed sample was filtered immediately by vacuum filtration through precombusted glass fiber filters. For the measurement of SS, each filter was dried for 2 hours at 105°C and then weighed. Taking into account the filtered volume, the increase in weight of the filter represented the total SS per unit volume (mg L^{-1}).

Daily SF, calculated from daily Q and SSC, was used to evaluate the model. Annual mean and seasonal variation of observed Q and SSC for 2000-2013 at these stations are presented in Table 2.

Table 2 Annual mean and seasonal variation of observed discharge (Q) and suspended sediment concentration (SSC) for 2000-2013 at 5 gauge stations.

2.3. Modelling approach

This study expands the work of Wei et al. (2019) where detailed descriptions of the modelling setup and the calibration and validation processes can be found. Here we only present some essential information about the modelling.

In the study of Wei et al. (2019), the daily simulated Q and SSC were presented. In this study, we dug and analyzed the outputs from the model, providing more information within this basin, such as the soil erosion which is an influencing factor for SF; and also we stated how the outputs from the modelling can be beneficial for the stakeholders.

2.3.1. The SWAT model

The Soil and Water Assessment Tool (SWAT) is a physically-based, semi-distributed hydrological model. It considers soils, land use and management conditions to predict the impact of land management practices on water and sediment within large complex basins where there might be no monitoring data over long periods of time (Neitsch et al., 2009).

Both hydrological and sediment dynamics in SWAT are simulated in two components: over the land, and in the channel network. More information about SWAT hydrological can be found in Arnold et al. (1998) and Neitsch et al. (2009).

To calculate the sediments from the landscape component, SWAT computes the erosion caused by rainfall with the Modified Universal Soil Loss Equation (MUSLE) for each HRU (Neitsch et al., 2009; Williams, 1975). This equation considers the surface runoff volume, peak runoff rate, soil erodibility, land cover and management, topographic and coarse fragment factor, as follows:

$$sed = 11.8 \cdot \left(Q_{surf} \cdot q_{peak} \cdot area_{hru}\right)^{0.56} \cdot K_{USLE} \cdot C_{USLE} \cdot P_{USLE} \cdot LS_{USLE} \cdot CFRG \quad (1)$$

where sed is the sediment yield on a given day (t), Q_{surf} is the surface runoff volume (mm H_2O ha^{-1}), q_{peak} is the peak runoff rate (m^3 s^{-1}), $area_{hru}$ is the area of the HRU (ha), K_{USLE} is the USLE soil erodibility factor which is related to the properties of the soil itself (0.013 ton m$_2$ hr/(m^3 ton cm)), C_{USLE} is the USLE land cover and management factor (defined as the ratio of soil loss from land cropped under specified conditions to the corresponding loss from clean-tilled, continuous fallow), P_{USLE} is the USLE support (agricultural) practice factor (defined as the ratio of soil loss with a specific support practice, such as contour tillage, strip cropping and terrace systems, to the corresponding loss with up-and-down slope culture), LS_{USLE} is the USLE topographic factor calculated according to the slopes of the basin, and CFRG is the coarse fragment factor.

The sediment routing in the channel is a function of two processes: deposition and degradation, operating simultaneously in the reach. The Simplified Bagnold equation (1977) is used as a default method for the sediment routing in stream channels which determines degradation as a function of channel slope and flow velocity. The maximum amount of sediment that can be transported is a function of the peak channel velocity, as follows:

$$conc_{sed,ch,mx} = c_{sp} \cdot v_{ch,pk}{}^{spexp} = c_{sp} \cdot \left(\frac{q_{ch,pk}}{A_{ch}}\right)^{spexp} = c_{sp} \cdot \left(\frac{prf \cdot q_{ch}}{A_{ch}}\right)^{spexp} \qquad (2)$$

where $conc_{sed,ch,mx}$ is the maximum concentration of sediment that can be transported by the water (t m^{-3}), c_{sp} is a coefficient defined by the user, $v_{ch,pk}$ is the peak channel velocity (m s^{-1}), spexp is an exponent defined by the user, $q_{ch,pk}$ is the peak flow rate (m^3 s^{-1}), A_{ch} is the cross-sectional area of flow in the channel (m^2), prf is the peak rate adjustment factor, and q_{ch} is the average rate of flow (m^3 s^{-1}).

2.3.2. SWAT data inputs

The topography, land cover and soil maps of the Red River basin for the model are presented here to give a better understanding of the characteristic of the Red River basin (Figure 2, Wei et al., 2019). The climate inputs including daily temperature and precipitation were obtained from remote sensing databases: Climate Forecast System Reanalysis (CFSR) and Tropical Rainfall Measuring Mission (TRMM, product 3B42 V7). The CFSR is a global, high resolution and reanalysis product, coupled atmosphere-ocean-land surface-sea-ice system designed to provide the best estimate of the state of these coupled domains over this period. CFSR, combining with hydrology models, has been proved to result in similar accuracy for computing Q as using surface observation data on large river basins (Dile and Srinivasan, 2014; Lauri et al., 2014). Simons et al. (2016) compared several satellite-based precipitation products to actual evapotranspiration products in the Red River basin and found that TRMM rainfall product could provide reliable values in both space and time at this basin. The resolutions and downloading sources of the above inputs can be found in the supplementary material (Table S-1).

Figure 2: (a) digital elevation model (gray shades); (b) slope classes: slopes were divided into 5 classes by SWAT based on the (DEM); (c) land use map; (d) soil types. Data sources are presented in the supplementary material (Table S-1), and the legends of land use and soil are detailed in the supplementary material (Tables S-2 and S-3).

2.3.3. Model set up

The whole basin was divided into 242 sub-basins by model based on 1) the characteristics of the basin according to the input data (DEM, soil property and land use); 2) the gauge stations and sampling sites; 3) dam locations; 4) harmonized size of all the sub-basins.

The main large dams in Table 1 were added to the model. In order to disentangle and quantify the impacts of the dams, two scenarios were simulated (Figure 3): (a) actual conditions with the existing dams; (b) reference scenario without dams. The difference between these two scenarios was the dam implementations. New dams mainly started to operate in 2008, therefore, the study period was divided into two sub-periods (pre-new-dams: 2000-2007 and post-new-dams: 2008-2013) to evaluate the total impact from old and new dams.

The hydrological parameters were kept the same for both periods (pre-new-dams and post-new-dams) for both the actual conditions and the reference scenario. Sediment parameters in Equation (1) and (2) were the same for pre-new-dams and post-new-dams periods except for the parameter c_{sp} which expresses the river bed erodibility. The dam implementations change the particle size distribution downstream, leading to a change in the channel erodibility (Wei et al., 2019). Therefore, c_{sp} was decreased from 0.008 for the pre-new-dams period to 0.002 for the post-new-dams period. For the reference scenario, the sediment parameters were kept the same as the pre-new-dams of the actual conditions. The sediment parameters setting is presented in Table S-4 in the supplementary material.

The simulation was carried out and calibrated on a daily scale from 2000 to 2013 and analyzed at different temporal scales (daily, monthly and annual).

Figure 3. Scenarios setting: actual conditions and reference scenario. Gray triangles are the old dams built before 2000 and black triangles are the new dams built after 2007.

2.3.4. Model evaluation and validation

Based on the daily-scale simulation, simulated monthly and annual SF were extracted to compare with observed data for checking the performance of the model. Following the recommendations by Moriasi et al. (2007), coefficient of determination (R^2), Nash–Sutcliffe Efficiency (NSE), and Percent Bias (PBIAS) were used to evaluate the simulations.

Results from the reference scenario were validated by comparing to the results from Lu et al. (2015), Vinh et al. (2014) and Dang et al. (2010).

2.4. Estimating the impacts of short-term climate variability and dams on SF

By comparing the mean annual SF of reference scenario between 2000-2007 and 2008-2013, the impacts of short-term climate variability can be quantified (Figure 3). By comparing the mean annual SF during 2008-2013 between actual conditions and reference scenarios, the impacts of dams can be quantified. By comparing the mean annual SF of actual conditions between 2000-2007 and 2008-2013, the impacts of four new dams and short-term climate variability can be quantified.

In this study, we hypothesized that the impact of the land use changes during our study period was not significant. Some researchers used a modelling approach to examine the impacts of land use changes on SF in Vietnam and found that an 11-16% decrease in forest land was likely to increase 3.0-3.9%

SF (Khoi and Suetsugi, 2014; Phan et al., 2010). In the Red River basin, between 2000 and 2010, the forest percentage stayed the same, and the farmland increased by 8% from bare land (Le et al., 2018), which might cause less than 2% increase of SF according to Khoi & Suetsugi (2014) and Phan et al. (2010). Therefore, we took into account the impact of land uses on SF but not of its changes during the study period.

2.5. Q-SF simple relationships

Another advantage of this modelling approach is that from the outputs of the modelling, the relationships (rating curves) between Q and SF can be inferred at any point within this basin, which enables people to estimate SF at any point with limited Q data. In this study, we would explore and present the relationships between monthly mean Q and SF for the 5 gauge stations as an example to show the benefits of this modelling. The results are presented in section 3.3. Different temporal scale relationships, such as daily or annual Q-SF relationships, can also be inferred by using the outputs of the modelling.

2.6. Identifying the influencing factors of soil erosion from landscape

The SS in the river can come from both hillslope soil erosion and channel processes. Therefore, having an insight into the land soil erosion can help people understand the source of the SS.

Hot spots of land soil erosion were identified according to the model outputs, and the main triggering factors were determined from the correlations between them and SF according to the principal component analysis (PCA) method described below.

PCA was used in this study to identify the factors influencing soil erosion in this basin. More detailed explanations of this method can be seen in Basilevsky (1994), Lever et al. (2017), Ringnér (2008) and Wold et al. (1987). Based on the parameters in Equation (1) and (2) and the analysis of parameters in the study of Wei et al. (2019), the following variables of each sub-basin were added into the PCA model to identify the main factor involved in SE in the basing: soil erosion (SE), precipitation (P), water yield (WY), surface runoff (SR), USLE soil erodibility factor (USLE_K), USLE agricultural practice factor (USLE_P), slope, and the percentages of sand (Sand%), silt (Silt%) and clay (Clay%) in soil. The input data to the PCA was the mean annual values of each variable of 242 sub-basins. Results about soil erosion hot spots and triggering factors are presented in section 3.4.

3. RESULTS

3.1. SF under actual conditions

3.1.1. Monthly variations of actual SF

Monthly and annual SF simulations and observations were plotted in Figure 4 and Figure 5, and their related statistics evaluations were reported in Table 3. From the general performance ratings at monthly scale recommended by Moriasi et al. (2007), Lao Cai, Yen Bai, Hoa Binh and Son Tay stations gained good performance; Vu Quang station gained satisfactory performance. PBIAS values indicate that the model slightly overestimated SF at most stations, and underestimated SF at Hoa Binh station.

Table 3 Evaluation statistics of sediment flux (SF) on different time scales for each station from 2000 to 2013

Thanks to the satisfactory calibration of Q and SSC presented in Wei et al. (2019), simulated SF shows similar trends as observed SF and can be considered as satisfactory results (Figure 4). Base flow of simulated monthly SF fits well with observations at all stations.

SF shows great seasonal variations, especially in the Thao River (see stations of Lao Cai and Yen Bai in Figure 4). Maximum flux usually occurs from July to September, and minimum flux generally happens from February and March. 87-91% of the annual total SF was produced during the flood season (May to October). The ranges of monthly SF variations and the values of mean monthly SF for flood and dry seasons at each station were summarized in Table 4. The Thao sub-basin has the highest SF and specific sediment yield (SSY) compared to the other two sub-basins and to the whole Red River basin.

Table 4 Seasonal variation of sediment fluxes and mean monthly sediment fluxes for flood and dry seasons at five gauge stations

Figure 4. Observed (black dot) and simulated (gray solid line) monthly sediment flux, and simulated sediment flux of reference scenario (without dams, gray dash line) at five stations from 2000 to 2013.

3.1.2. Annual variations of actual SF

The annual SF exhibits different temporal and spatial variations among the 5 gauge stations (Figure 5). For the Thao River, the simulated annual SF ranged from 6.8 to 73.6 Mt yr^{-1} at Lao Cai (with 30.7 Mt yr^{-1} on average during 2000-2013, Table 5), and from 11.7 to 85.9 Mt yr^{-1} at Yen Bai (39.8 Mt yr^{-1} on average). The Lo River at Vu Quang is predicted to produce SF ranging from 2.0 to 12.5 Mt yr^{-1} (with 6.6 Mt yr^{-1} on average). On the Da River at Hoa Binh station, the minimum annual SF was 0.8 Mt yr^{-1} and the maximum was 7.1 Mt yr^{-1} (with 3.6 Mt yr^{-1} on average). Amongst these three tributaries, the Thao River produces the highest SF, followed by the Lo River, and the Da River generates the lowest SF. The Thao River shows higher SF than the other two tributaries due to its high SSC (the annual mean SSC during 2000-2013 at Lao Cai and Yen Bai were 1057 and 1003 mg L^{-1}, respectively, Wei et al., 2019). Even though SSC at Hoa Binh station on the Da River (the annual mean SSC during 2000-2013 was 57 mg L^{-1}, Wei et al., 2019) is much smaller than at Vu Quang on the Lo River (the annual mean SSC during 2000-2013 was 172 mg L^{-1}, Wei et al., 2019), the SF of these two rivers are in the same range. The Da River has a larger runoff (the annual mean Q during 2000-2013 was 1362 m^3 s^{-1}, Wei et al., 2019) with low SSC induced by dam retention, while the Lo River has a lower runoff (the annual mean Q during 2000-2013 was 729 m^3 s^{-1}, Wei et al., 2019) with a higher SSC. As the confluence of these tributaries, the Red River (at Son Tay station) yields an annual SF at the range of 8.0-69.2 Mt yr^{-1}, with an average specific sediment yield (SSY) of 240.3 t km^{-2} yr^{-1} over

2000-2013 (357.6 t km^{-2} yr^{-1} over 2000-2007 and 84.5 t km^{-2} yr^{-1} over 2008-2013).

Figure 5. Annual sediment flux (SF) variation from 2000-2013 at 5 gauge stations, and the mean annual SF of pre-new-dams (2000-2007) and post-new-dams (2008-2013). The annual precipitation variation of the whole basin from 2000-2013.

The values of mean annual SF during the study period and sub-periods from references are displayed in Table 5. For the whole study period, simulated mean annual SF shows a good match with in-situ data, though slight overestimation at Yen Bai and Son Tay stations. By comparing the mean annual SF of 2008-2013 between reference scenario and actual conditions, the mean annual sediment trapped by the dams during this period ranged from 7.1 Mt yr^{-1} (Lo River) to 111.0 Mt yr^{-1} (Da River).

Table 5 Simulated sediment flux (Mt yr^{-1}) of reference scenario (without dams) and actual conditions (over the whole study period, 2000-2007 period and 2008-2013 period) compared with other studies and in-situ data; values of trapped sediment (calculated as the difference between average values over 2008-2013 in the reference scenario and actual simulations); impacts of short-term climate variability and dams.

AC[†]: Actual Conditions

RS[‡]: Reference Scenario (without dams)

3.2. SF of reference scenario (without dams)

3.2.1. Inter-annual variations

Like the actual SF (Figure 5), interannual SF of reference scenario (without dams) exhibits high variations. During the study period, results from reference scenario suggest that annual SF at Lao Cai, Yen Bai, Vu Quang and Hoa Binh stations should have been from 21.3 to 73.6 Mt yr^{-1}, 29.6 to 90.7 Mt yr^{-1}, 6.9 to 15.8 Mt yr^{-1}, 81.5 to 191.0 Mt yr^{-1}, respectively, thus with a factor of 3 between the highest and the lowest values in the Thao River, and a factor of 2.3 in the Lo and Da rivers. According to the results at the outlet (Son Tay station) the Red River basin should have exported 69.6 to 170.7 Mt yr^{-1} of sediment, with an average SSY of 778.8 t km^{-2} yr^{-1} over 2000-2013.

3.2.2. Mean annual SF

Annual SF of reference scenario was compared with observed data from references (Dang et al., 2010; Lu et al., 2015; Vinh et al., 2014, Table 5) which covered periods preceding the dams constructions, i.e. before 1979. Despite different periods, the simulations without dams for most stations (except Hoa Binh station) are close to those in-situ data. At Son Tay, the simulation without dams is slightly lower (~10%) than those reference data. These comparisons show that the model produces an acceptable simulation of SF without dams.

3.3. Simple Q-SF relationship under actual conditions

By using the outputs of the modelling, the simple relationships between Q and SF can be inferred at any point within the Red River and any temporal scales. As monthly mean Q data can be more easily accessed or gained, therefore, here we inferred the monthly mean Q-SF rating curves at the five gauge stations as an example.

For both the 2000-2007 and 2008-2013 periods, monthly simulated SF of actual conditions showed a positive power-law relation with monthly simulated Q for the 5 gauge stations as shown by fitted curves in Figure 6, with R^2 above 0.96. These 5 stations exported less SF after 2008, which highlights the changes caused by short-term climate variability and by sediment retention of dams. We, therefore, established separately power-law relationships between simulated Q and SF for both periods before and after 2008.

Figure 6. Correlation and relations between simulated monthly mean discharge (Q) and simulated monthly mean sediment fluxes (SF) at 5 stations in the simulation under actual conditions. Gray solid squares are of the period 2000-2007; gray hollow squares are of the period 2008-2013. Black solid and dash lines are the fitting curves of the period 2000-2007 and 2008-2013, respectively.

3.4. Hot spots of soil erosions

The SWAT model can not only be used to simulate, study and assess the in-stream SF, but also the sediment erosion from the land component. Then, based on these simulated mean annual sediment fluxes and soil erosion, hot spots of erosion were identified and presented in Figure 7c.

The model results indicate that the mean annual soil erosion in the whole basin ranged from 0.01 to 43.4 t ha^{-1} yr^{-1}, with a mean of 5.5 t ha^{-1} yr^{-1} (Figure 7c), and the mean annual soil erosion of the Red River basin during 2000-2013 was 64.0 Mt yr^{-1}. High erosion areas are identified in the middle part of the Thao River and the downstream of the Da River: with high precipitation (>1500 mm yr^{-1}, Figure 7a) and surface runoff (>450 mm yr^{-1}, Figure 7b), Lai Chau (sub-basin 173), Lao Cai (sub-basins 116, 117, 135, 148, 149, 157), Ha Giang (sub-basin 119) and Son La (sub-basins 218, 232, 234, 237, 240, 241) provinces are the most vulnerable to soil erosion, and their mean annual erosion rate during the study period can be above 20 t ha^{-1}.

Figure 7d presents the in-stream SF spatial variations. High SF can reach locally above 80 t yr^{-1}, with hot spots of high values identified upstream of the Hoa Binh dam, which corresponds with the annual SF values before Hoa Binh dam construction (Table 5).

Figure 7. Mean annual value of (a) Precipitation distribution (mm yr^{-1}), (b) Surface Runoff (mm yr^{-1}), (c) Soil Erosion (ton ha^{-1} yr^{-1}), (d) In-stream Sediment Flux (ton yr^{-1}) within 242 sub-basins, derived from the actual conditions simulation over the period 2000-2013.

Principal component analysis (PCA) was applied to identify the factors influencing soil erosion (Table 6). The PCA results based on the correlation matrix analysis with Varimax rotation produce 3 principal components (PCs) with eigenvalues greater than 1.00, corresponding to an overall cumulative variance of 78.3%, moreover, the 2 first PCs represent a cumulated variance of

67.5%.

Table 6 The principal component (PC) loading

†: the simulation from the model

‡: the observation and input data

Notes: underlined values correspond to the first three highest factor loadings in the PC.

4. DISCUSSION

4.1. Uncertainties

Differences between simulations and observations are large on some peaks of SF flow: during these peaks, the SF can be underestimated by a factor >2 (Figure 4). Uncertainties can come from three factors: uncertainties associated with rainfall satellite input data; errors due to the numerical simulation approximations; uncertainties associated with in-situ measurement errors on Q and SSC.

Previous studies indicated that the TRMM (satellite rainfall dataset) underestimated the rainfall when there were intensive or extreme rainfall events (Le et al., 2014; Liu et al., 2015; Simons et al., 2016). The underestimations on rainfall values can cause underestimations in Q simulation which might induce underestimations in channel erosion and re-suspended processes (Wei et al., 2019) and also in soil erosion.

Some studies indeed showed that modelling might underestimate SSC during high and intensive rainfall (Oeurng et al., 2011; Xu et al., 2009). Modelling errors can come from the simplification of algorithms. For example, in SWAT, for land erosion SWAT model uses a runoff factor instead of rainfall energy factor (Equation 1); and for the channel processes, SWAT uses a simplified version of Bagnold stream power equation to calculate the maximum amount of sediment that could be transported in a stream segment (Equation 2, Bagnold, 1977; Neitsch et al., 2009). However, this algorithm does not keep track of particle size distribution of elements that pass through the channel, and sediments all are assumed to be of silt size. Besides, the channel erosion is not partitioned between stream bank and bed, and deposition is assumed to occur only in the main channel; flood plain sediment deposition is also not modelled separately (Neitsch et al., 2009). Therefore, this simplification can cause deviations for sediment routing.

In-situ measurements and sampling strategy can also cause errors. For example, a high sampling frequency enables to diminish errors in the estimation of annual SF (Dang et al., 2010). Q and SSC measurements during flood events are usually extrapolated by the rating curve. However, the fact that those rating curves may have been established based on non-exceptional conditions might cause deviations on both Q and SSC, and consequently on SF.

Besides the above main factors, irrigation diversion and sand excavation can also affect suspended sediment transfer. However, no available data to quantify their impacts on SF of the Red River. Future studies should fill this gap.

4.2. SF variations caused by short-term climate variability

Comparing the annual SF of reference scenario (without dams) between 2008-2013 and 2000-2007 shows that short-term climate variability has different impacts on these tributaries, though it induces a decrease at most stations, except at Vu Quang (Table 5 and Figure 5). The biggest impacts are observed at the two stations on the Thao River (Lao Cai and Yen Bai), causing an average 25% decrease of SF, followed by the Da River (Hoa Binh, ~-10%), with a resulting ~10% decrease on the Red River (Son Tay). On the contrary, at Vu Quang station, the mean annual SF very slightly increased by 2%, in accordance with a similar Q change (2%, Wei et al., 2019).

In order to figure out the different responses of each tributary to short-term climate variability, we compared the rainfall and water availability (the difference between rainfall and evapotranspiration) variations between 2008-2013 and 2000-2007, and the variations are presented in Figure 8. In the upper and middle parts of the Red River basin, both rainfall and water availability decreased while the lower part showed an increasing tendency. At sub-basin scale, the variations of the rainfall were -9% for the Thao basin, +2% for the Lo basin and -2% for the Da basin; for water availability, the Thao and Da basins decreased by 13% and 4%, respectively, while the Lo basin increased by 7%. The impacts of short-term climate variability on SF for each sub-basin are in accordance with the variations of rainfall and evapotranspiration: the Thao river showed the largest reduction while the Lo river showed an increase.

Previous studies revealed that climate variability had an effect on both Q and SSC in the Red River basin (Wei et al., 2019), and suggested a decrease of rainfall mean and extremes over the last decades over Southeast Asia (Manton et al., 2001). A 14-year period is not long enough for detecting the climate variability on SF, therefore, this study only aimed at discovering the different responses of each subbasin to the short-term climate variability during the study period, and does not make conclusions for climate changes and the tendency for the future. Longer periods of study are needed to study the climate trends and variability effects on SF. The SF trend of the Red River under the influence of long-term climate variability and hydrology changes will be carried out in future studies based on the methodology proposed by this study.

Figure 8. The differences in annual rainfall (a) and annual water availability (b) between 2008-2013 and 2000-2007.

4.3. Impacts of dams

4.3.1. The reduction caused by dams

Among the three tributaries, dams' impact on the outlet of the Da River (Hoa Binh station) is the most severe, followed by the Lo River; and the dams are less affected on the Thao River (Table 5). Two new dams in China caused around a 48% reduction of SF on the Thao River. More cascade dams are under construction in China, so this value can provide a reference for future studies. The dams on the Lo River reduced around 74% of the annual SF. The large dams on the Da River show an enormous impact on SF, and the trap efficiency is 89% compared to 86-91% from other studies which did not estimate the specific impacts of climate variations of different periods and neither the impact of the Son La dam (Dang et al., 2010; Vinh et al., 2014). At the outlet of the Red River basin, the dams upstream caused an 80% decrease of annual SF.

The Son La and Hoa Binh dams on the Da River have large capacities and are located quite downstream to the outlet of the river compared to the dams on the other two tributaries, explaining their higher relative impact. The capacities of the Thac Ba and Tuyen Quang dams are also larger than the two dams on the Thao River. The two dams (Nansha and Madushan) on the Thao River are above 100 km upstream of the Yen Bai station, and along the reach between the dams and Yen Bai station, the impacts of dams on sediment transport are mitigated by the degradation and the soil erosion from the land component. Therefore, the dams show larger impact at the outlet of the Lo River than the Thao River.

Previous studies (Dang et al., 2010; Lu et al., 2015; Vinh et al., 2014) used long-term observed Q and SSC data to analyse the impact of dams on SF. Dang et al. (2010) analysed the observed Q and SSC from 1960-2008, but only at Son Tay station, did not study the Lo and the Da rivers; Vinh et al. (2014) analysed the observed data from 1960-2010 at four stations (not in Lao Cai) and focused the analysis on the impact of the Hoa Binh dam; Lu et al. (2015)

also used the observed data from 1960-2010 to assess the impact of a sequence of dams but without considering the dams upstream in China. This study revisits the impacts of dams by taking into account more dams recently built in the Red River basin. With more dams implemented after 2013 or planned at short/mid-term on these three tributaries, the sediment trap efficiency might still increase and the SF decreases at the outlet of each tributary, consequently at the outlet of the Red River.

4.3.2. Impacts on dynamic processes

From the seasonal variation of SF (Figure 4), it can be noticed that the flow curve (dynamic processes) with and without dams are similar; the impacts of dams are significant on SF peak flow during flood seasons, and dams have much fewer impacts on the base flow of SF.

However, the impacts on the dynamic processes at each station can be different. For example, in 2008, the simulation without dams seems to fit the observations better at Yen Bai and Vu Quang than at other stations. This suggests that, on the same river (Thao), the Nansha dam had weaker impacts at Yen Bai (located more downstream, Figure 1) than at Lao Cai for the first year of dam operation, and it can be related to the sediment degradation processes between Lao Cai and Yen Bai. Also, the Tuyen Quang dam only slightly impacted SF at Vu Quang for the first year of implementation, presumably because the Lo River has much less SS than the other two tributaries and the sediment retention caused by the new dam at the first year can be relatively lighter. Besides, the Tuyen Quang dam is located on one tributary of the Lo River, whereas the other dams are located directly in the main branch of the Thao and Da rivers. Therefore, the Tuyen Quang dam on the Lo River has smaller impacts on sediment transport. In addition, the operation scheme of these new dams can be also a reason that induces different impacts on SS dynamic processes as different discharge releases can carry different amounts of sediment, and discharge release of each dam depends on the main function (flood control or irrigation or power generation) of this dam and its capacity (Wang et al., 2017).

4.4. Soil erosion

The PCA results identified the factor loadings of each component (Table 6): PC1 (consisted of precipitation (P), water yield (WY) and surface runoff (SR)) has the highest weighted variable (41.6%), followed by PC2 (25.9%) which is consisted of soil erosion (SE), slope and USLE agricultural practice factor (USLE_P), and PC3 (10.8%, the percentage of sand (Sand%), silt (Silt%) and clay (Clay%) in soil, i.e. the soil texture). Therefore, precipitation (as water yield and surface runoff are fractions of precipitation), slope and USLE agricultural practice factor (USLE_P) are key influence factors for soil erosion in the Red River basin. The soil texture is also a significant factor. Our results are in agreement with He et al. (2007) who indicated that human activities and climate change are the major influences to the sediment change in the mountainous upstream area in China and Ranzi et al. (2012) who highlighted the major role of rainfall in soil erosion in the Lo basin; Yang et al. (2003) found that the hot spots of soil erosion in Southeast Asia were close mountainous areas located in the tectonic zones and dense croplands regions where both natural geomorphology and human activity are major factors for inducing soil erosion. In the middle part of the Ren River basin (especially in the Thao and Da subbasins), agricultural activities are distributed in these mountain areas with steep slopes, and terrace systems and contour farming are popular. Therefore, in these hot spots of soil erosion, agricultural practices on steep mountain areas should be paid attention. With more forests might be converted to farmland in the future, soil erosion might be increased.

In the upper Red River basin in China, the soil erosion area accounted for ~44% of the total basin area in China, with a soil modulus of 14.8 t ha^{-1} yr^{-1} (He et al., 2007). Tuan et al. (2014) found annual soil losses from 1.8 to 174 t ha^{-1} yr^{-1} from plot-scale experiment near Son La. Podwojewski et al. (2008) found a soil erosion from 0.86 to 13.5 t ha^{-1} yr^{-1} also in Hoa Binh province on steep slopes. Based on a RUSLE model, Nguyen et al. (2012) simulated a continuous increase of the soil erosion from 1970 to the recent decade 2000, from 4.9 to 5.9 t ha^{-1} yr^{-1}. Mai et al. (2013) found a 1.63 to 17.22 t ha^{-1} yr^{-1} erosion rate near Son Tay. Our simulation is in the range of these references: from 0.01 to 43.4 t ha^{-1} yr^{-1}, with a mean of 5.5 t ha^{-1} yr^{-1} over the whole basin.

The soil of the high erosion areas - the middle part of the Thao River and the downstream of the Da River (Figure 7c) - is mainly composed of Orthic Acrisols (Ao90-2-3c-4284, Figure 2c and Table S-3). This type of soil is acid with sandy-loamy surface soil, and prone to slaking, crusting and erosion. Acrisols form the tropical red soils and red earths, and after eluviation they are subjected to erosion (FAO, 2003). This result is in agreement with the above conclusion obtained from PCA.

Estimates of annual SF show that Yen Bai produces more SF than Lao Cai (~30% over the whole period, both under reference scenario and actual conditions, Figure 5). This indicates that the soil erosion or/and resuspension likely happens in the part of the basin between Lao Cai and Yen Bai. This can be confirmed by the spatial identification of soil erosion (Figure 7c) which also indicates that Lao Cai province is a hot spot of soil erosion.

Before the construction of Hoa Binh dam, sediment input to the Red River mainly originated from the Da River (~120 Mt yr^{-1} in the reference scenario simulations, i.e. more than twice the values estimated for the other tributaries, Table 5). The high in-stream SF of the Da River results from both land erosion and channel degradation. Complex dam regulation can cause complex hydraulics compared to the natural channel. Comparison of the reference scenario (without dams) and actual conditions simulations over the period 2008-2013 suggests a 111 Mt yr^{-1} value of trapped sediment at the Hoa Binh dam. Such a big quantity of sediment from upstream of Hoa Binh should catch the attention of the management because big sedimentation in the reservoir would reduce the capacity and performance of the dam. As explained in section 2.1.4, this is also a reason why the Son La dam was built.

4.5. Comparison with other basins

To compare our results with SF and specific sediment yield (SSY) without dams obtained for other Asian rivers, the values provided by Milliman and Syvitski (1992) were considered since they were obtained before 1992 and are less impacted by dams than more recent estimates provided by the literature. From our simulation of reference scenario (without dams), the Red River yields an annual SF of 107 Mt yr^{-1}, corresponding to a SSY of 780 t km^{-2} yr^{-1} (Table 5). The Yellow River produced 1100 Mt yr^{-1} SF with a SSY of 1400 t km^{-2} yr^{-1}; the Yangtze River caused 480 Mt yr^{-1} SF with a SSY of 250 t km^{-2} yr^{-1}; the Pearl River generated 69 Mt yr^{-1} SF with a SSY of 160 t km^{-2} yr^{-1}; the Mekong River yielded 160 Mt yr^{-1} SF with a SSY of 200 t km^{-2} yr^{-1} (Milliman and Syvitski, 1992). The Red River basin without dams thus exported less SF than the Yellow River (-90%), the Yangtze River (-78%) and the Mekong River (-33%), and 55% more than the Pearl River. However, its SSY was higher than the Mekong (+290%), Pearl River (+388%), Yangtze (+212%), and nearly half of the Yellow River (-44%). When compared to an equivalent surface watershed such as the upper Danube (132,000 km^2), the Red River basin produced almost 3 times higher SSY than that of 265 t km^{-2} yr^{-1} generated by the upper Danube; besides, the upper Danube basin only exported 21.2 t km^{-2} yr^{-1} to the downstream part (Vigiak et al., 2015). These results show that without impacts of dams, the Red River basin, though having a smaller surface than the other basins in the world, would be a very large source of suspended sediments to the sea due to its soil erosion caused by active tectonic movements, steep slopes, deep valleys, high precipitation and intensive agricultural activities along the upstream river (Le et al., 2017, 2007).

4.6. Interpretation of Q-SF simple relations

From Figure 6, we can see that the relation between monthly Q and SF is a power-law relation of the form:

$$\mathrm{SF} = \mathrm{a}Q^{b} \tag{3}$$

where SF is the monthly mean sediment flux (t day^{-1}), Q is monthly mean water discharge (m^3 s^{-1}), *a* and *b* are regression coefficients.

Equation (3) is formally in accordance with a general sediment rating curve (Asselman, 2000; Syvitski et al., 2000):

$$\mathrm{SSC} = a'Q^{b'} \tag{4}$$

where SSC is the suspended sediment concentration (mg L^{-1}), *a'* and *b'* being the regression coefficients. The coefficient *a'* represents the erodibility of the soil, and is equal to SSC when Q is 1 m^3 s^{-1}; a sub-basin with intensively weathered materials which can be eroded and transported easily usually shows a high value of the coefficient *a'*. The coefficient *b'* represents the erosive power of the river and the transport capacity; it is also affected by the grain size distribution of the material available for transport: rivers with sand-sized sediments have higher *b'* values than rivers with silt and clay-sized sediments.

As discussed before, among the three sub-basins, the Thao and Da sub-basins present steep slopes and are vulnerable to soil erosion, therefore their *a*-coefficient should be high. The two stations on the Thao River have the highest *a* values (Figure 6); however, the Hoa Binh station on the Da River has the lowest *a* value among these three tributaries because the eroded soil was retained in the Hoa Binh dam. For each station, the *a*-value decreased between 2000-2007 and 2008-2013 (Figure 6): dams retain the SS from upstream soil erosion which induces a decrease of *a* value downstream of the dam.

The average values of the median diameter D_{50} of surface sediment before new dam constructions are 0.16, 0.35, 0.175 and 0.2 mm in the Thao, Da, Lo rivers and the reach between the confluence of the Da and Thao rivers at Son Tay, respectively (Vinh et al., 2014), and there is a relationship between the parameter *b* (over the period 2000-2007, before new dams) and the values of the median diameter D_{50} of surface sediment before new dam constructions (Figure 9). The *b* values during 2000-2007 are similar at Lao Cai and Yen Bai on the Thao river and at Vu Quang on the Lo river (from 1.61 to 1.65, Figure 6), but not during 2008-2013 (1.79 at Lao Cai and Yen Bai vs.1.59 at Vu Quang). The differences of the b values between 2000-2007 and 2008-2013 can indicate that the dams on the Thao and Lo rivers might change the grain size distributions and transport capacity at these stations: new dam constructions may have induced a higher (with *b* increasing) median diameter D_{50} of surface sediment in the Thao river while a lower one (with *b* decreasing) in the Lo river.

Figure 9. Relationship between the parameter *b* and the values of the median diameter D50 of surface sediment

The coefficients *a* and *b* in the simple Q-SF equation are in agreement with the real sub-basin characteristics. The curves of two periods also illustrate the differences of the sediment regimes during these two periods: curves of 2008-2013 are gentler than of 2000-2007 (Figure 6), i.e. under the same Q, the SF is lower compared to 2000-2007, which is due to a combined impact of climate and dams. Also, the outputs from the model can be used to infer Q-SF relationship at any other point within this basin. Hence, these simple Q-SF equations can be used by stakeholders to estimate the monthly SF without using the SWAT model.

5. CONCLUSIONS

This study aimed to characterize the suspended sediment flux and the soil erosion of the Red River basin by using the outputs of a numerical model and in-situ data. Suspended sediment flux was quantified based on daily simulations of discharge and suspended sediment concentration during a long period, taking into account the successive implementations of dams and the short-term climate variability during this period. Furthermore, by implementing a reference scenario (without dams in this basin), this study allowed to disentangle the impacts of short-term climate variability and damming at the outlets of each main tributary as well as at the outlet of the continental basin. This provides a reference for future studies on dams' functions and water resource management.

Under the main influence of damming, the suspended sediment fluxes showed a drastic decrease during 2008-2013 compared to 2000-2007. These two influencing factors had different effects on each sub-basin. Due to the different climatic characteristics, such as precipitation distribution and variation, the Thao River is more sensitive to short-term climate variability than the other two tributaries. Conversely, the Da River is the most affected by constructions of huge-capacity dams. At the outlet of the Red River basin, the mean annual sediment fluxes decreased by 90% compared to the value estimated from reference scenario (without dams) during 2000-2007, of which 10% was due to short-term climate variability and 80% to the dams. A power-law relation between monthly mean discharge and sediment flux was provided at each outlet of the main tributaries and the Red River for stakeholders and decision-makers to have an easy tool to estimate the sediment flux.

The high advantage of the model, once it has been calibrated with data from hydrological stations, is that it can serve to estimate and map each term involved in the sediment transport process – including local erosion, local deposition, in-stream sediment discharge, etc. – and that it can be used to infer local SF-Q rating curves at any virtual station within the basin from the model simulations, even where there is no true station. This point is of major interest both for scientific applications (e.g., studying spatial variations of SF) and for management purposes, with provinces and other stakeholders.

Land management (such as agricultural practice) should pay attention on the high soil erosion areas located in the middle part of the Thao sub-basin and the lower part of the Da sub-basin due to the precipitation distribution, topography and soil texture, and river management should notice the sediment retained in the dams on the Da River.

Some improvements can be done in future research. This study hypothesized that the impact of the land use changes was not significant during our study period and did not take into account the impacts of land use changes on soil erosion and sediment flux. In the future, more forests might be converted into farmland in this basin, therefore, it would be interesting to evaluate the impacts of land use change on sediment fluxes. A more precise and higher-frequency in-situ dataset would be useful, such as longer and high-frequency hydrological and meteorological data at more stations, and more information about dam management, in order to have a better estimation and understanding of the impacts of climate variability and human interferences.

With on-going and future climate change and dam constructions in this basin, it would be necessary to pursue further research about the sediment flux variation and its associated contaminant fluxes as well as carbon transfer in order to better manage this basin and protect the downstream coastal areas. In addition, running numerical simulations under scenarios of global changes, such as land use changes and urbanization, would allow us to estimate the impacts of these changes on hydrology and suspended sediment fluxes.

ACKNOWLEDGEMENT:

This research was developed in the framework of the Land-Ocean-aTmosphere regional coUpled System study center (LOTUS), an international joint Vietnamese/French laboratory (http://lotus.usth.edu.vn/) funded by the Institut de Recherche pour le Développement (IRD). We thank LOTUS for providing the dataset, and also the research travel funds for Xi Wei to collect data and information in Vietnam. The PhD scholarship of Xi Wei is financially supported by the China Scholarship Council (CSC), grant number 201606240088.

CONFLICTS OF INTEREST:

The authors declare that no conflict of interest could be perceived as prejudicing the impartiality of the research reported.

References:

Arias, M.E., Cochrane, T.A., Kummu, M., Lauri, H., Holtgrieve, G.W., Koponen, J., Piman, T., 2014. Impacts of hydropower and climate change on drivers of ecological productivity of Southeast Asia's most important wetland. Ecol. Modell. 272, 252–263. https://doi.org/10.1016/j.ecolmodel.2013.10.015

Arnold, J.G., Srinivasan, R., Muttiah, R.S., Williams, J.R., 1998. Large area hydrologic modeling and assesment Part I: Model development. JAWRA J. Am. Water Resour. Assoc.

34, 73–89. https://doi.org/10.1111/j.1752-1688.1998.tb05961.x

Asselman, N.E.M., 2000. Fitting and interpretation of sediment rating curves. J. Hydrol. 234, 228–248. https://doi.org/10.1016/S0022-1694(00)00253-5

Bagnold, R.A., 1977. Bed load transport by natural rivers. Water Resour. Res. 13, 303–312. https://doi.org/10.1029/WR013i002p00303

Bai, Z., Feng, D., Ding, J., Duan, X., 2015. A study on the variations of soil physico-chemical properties and its environmental impact factors in the Red River watershed (in Chinese). Yunnan Geogr. Environ. Res. 27, 81–90. https://doi.org/10.13277/j.cnki.jcwu.2015.04.013

Barton, A.P., Fullen, M.A., Mitchell, D.J., Hocking, T.J., Liu, L., Wu Bo, Z., Zheng, Y., Xia, Z., 2004. Effects of soil conservation measures on erosion rates and crop productivity on subtropical Ultisols in Yunnan Province, China. Agric. Ecosyst. Environ. 104, 343–357. https://doi.org/10.1016/j.agee.2004.01.034

Basilevsky, A., 1994. Statistical Factor Analysis and Related Methods-Chapter 3: The Ordinary Principal Components Model, Wiley Series in Probability and Statistics. John Wiley & Sons, Inc., Hoboken, NJ, USA. https://doi.org/10.1002/9780470316894

Beusen, A.H.W., Van Beek, L.P.H., Bouwman, A.F., Mogollón, J.M., Middelburg, J.J., 2015. Coupling global models for hydrology and nutrient loading to simulate nitrogen and phosphorus retention in surface water - Description of IMAGE-GNM and analysis of performance. Geosci. Model Dev. 8, 4045–4067. https://doi.org/10.5194/gmd-8-4045-2015

Chen, J., Shi, H., Sivakumar, B., Peart, M.R., 2016. Population, water, food, energy and dams. Renew. Sustain. Energy Rev. 56, 18–28. https://doi.org/10.1016/j.rser.2015.11.043

Cohen, S., Kettner, A.J., Syvitski, J.P.M., 2014. Global suspended sediment and water discharge dynamics between 1960 and 2010: Continental trends and intra-basin sensitivity. Glob. Planet. Change 115, 44–58. https://doi.org/10.1016/j.gloplacha.2014.01.011

Dai, S.B., Yang, S.L., Li, M., 2009. The sharp decrease in suspended sediment supply from China's rivers to the sea: Anthropogenic and natural causes. Hydrol. Sci. J. 54, 135–146. https://doi.org/10.1623/hysj.54.1.135

Dang, T.H., Coynel, A., Orange, D., Blanc, G., Etcheber, H., Le, L.A., 2010. Long-term monitoring (1960-2008) of the river-sediment transport in the Red River Watershed (Vietnam): Temporal variability and dam-reservoir impact. Sci. Total Environ. 408, 4654–4664. https://doi.org/10.1016/j.scitotenv.2010.07.007

Dang, T.H., Ouillon, S., Van Vinh, G., 2018. Water and Suspended Sediment Budgets in the Lower Mekong from High-Frequency Measurements (2009–2016). Water 10, 846. https://doi.org/10.3390/w10070846

Dile, Y.T., Srinivasan, R., 2014. Evaluation of CFSR climate data for hydrologic prediction in data-scarce watersheds: an application in the Blue Nile River Basin. JAWRA J. Am. Water Resour. Assoc. 50, 1226–1241. https://doi.org/10.1111/jawr.12182

FAO, 2011a. The state of the world's land and water resources for food and agriculture (SOLAW) – Managing systems at risk, Food and Agriculture Organization of the United Nations, Rome and Earthscan, London. Food and Agriculture Organization of the United Nations, Rome and Earthscan, London.

FAO, 2011b. Irrigation in Southern and Eastern Asia in figures, AQUASTAT Survey – FAO Water report 37.

FAO, 2003. Multilingual Thesaurus on Land Tenure (Chinese version).

Furuichi, T., Win, Z., Wasson, R.J., 2009. Discharge and suspended sediment transport in the Ayeyarwady River, Myanmar: centennial and decadal changes. Hydrol. Process. 23, 1631–1641. https://doi.org/10.1002/hyp.7295

Hauer, C., Leitner, P., Unfer, G., Pulg, U., Habersack, H., Graf, W., 2018. The Role of Sediment and Sediment Dynamics in the Aquatic Environment, in: Riverine Ecosystem Management. Springer International Publishing, Cham, pp. 151–169.

https://doi.org/10.1007/978-3-319-73250-3_8

He, D., Ren, J., Fu, K., Li, Y., 2007. Sediment change under climate changes and human activities in the Yuanjiang-Red River Basin. Chinese Sci. Bull. 52, 164–171. https://doi.org/10.1007/s11434-007-7010-8

Hiep, N.H., Luong, N.D., Viet Nga, T.T., Hieu, B.T., Thuy Ha, U.T., Du Duong, B., Long, V.D., Hossain, F., Lee, H., 2018. Hydrological model using ground- and satellite-based data for river flow simulation towards supporting water resource management in the Red River Basin, Vietnam. J. Environ. Manage. 217, 346–355. https://doi.org/https://doi.org/10.1016/j.jenvman.2018.03.100

IPCC, 2019. Special Report on climate change, desertification, land degradation, sustainable land management, food security, and greenhouse gas fluxes in terrestrial ecosystems. The Intergovernmental Panel on Climate Change. Geneva, Switzerland.

Jiang, T., Fischer, T., Lu, X., 2009. Larger Asian rivers: Climate change, river flow, and watershed management. Quat. Int. 208, 1–3. https://doi.org/10.1016/j.quaint.2010.06.011

Khoi, D.N., Suetsugi, T., 2014. The responses of hydrological processes and sediment yield to land-use and climate change in the Be River Catchment, Vietnam. Hydrol. Process. 28, 640–652. https://doi.org/10.1002/hyp.9620

Kunz, M.J., Wüest, A., Wehrli, B., Landert, J., Senn, D.B., 2011. Impact of a large tropical reservoir on riverine transport of sediment, carbon, and nutrients to downstream wetlands. Water Resour. Res. https://doi.org/10.1029/2011WR010996

Lal, R., Kimble, J., Levine, E., Stewart, B.A., 1995. Soils and global change. CRC Press, Boca Raton, USA.

Lauri, H., Räsänen, T.A., Kummu, M., 2014. Using Reanalysis and Remotely Sensed Temperature and Precipitation Data for Hydrological Modeling in Monsoon Climate: Mekong River Case Study. J. Hydrometeorol. 15, 1532–1545. https://doi.org/10.1175/JHM-D-13-084.1

Le, T.B., Al-Juaidi, F.H., Sharif, H., 2014. Hydrologic simulations driven by satellite rainfall to study the hydroelectric development impacts on river flow. Water (Switzerland) 6, 3631–3651. https://doi.org/10.3390/w6123631

Le, T.P.Q., 2005. Biogeochemical Functioning of the Red River (North Vietnam): Budgets and Modelling. Université Paris VI- Pierre et Marie Curie.

Le, T.P.Q., Dao, V.N., Rochelle-Newall, E., Garnier, J., Lu, X., Billen, G., Duong, T.T., Ho, C.T., Etcheber, H., Nguyen, T.M.H., Nguyen, T.B.N., Nguyen, B.T., Da Le, N., Pham, Q.L., 2017. Total organic carbon fluxes of the Red River system (Vietnam). Earth Surf. Process. Landforms 42, 1329–1341. https://doi.org/10.1002/esp.4107

Le, T.P.Q., Garnier, J., Gilles, B., Sylvain, T., Van Minh, C., 2007. The changing flow regime and sediment load of the Red River, Viet Nam. J. Hydrol. 334, 199–214. https://doi.org/10.1016/j.jhydrol.2006.10.020

Le, T.P.Q., Le, N. Da, Dao, V.N., Rochelle-Newall, E., Nguyen, T.M.H., Marchand, C., Duong, T.T., Phung, T.X.B., 2018. Change in carbon flux (1960–2015) of the Red River (Vietnam). Environ. Earth Sci. 77, 658. https://doi.org/10.1007/s12665-018-7851-2

Lehner, B., Liermann, C.R., Revenga, C., Vörösmarty, C., Fekete, B., Crouzet, P., Döll, P., Endejan, M., Frenken, K., Magome, J., Nilsson, C., Robertson, J.C., Rödel, R., Sindorf, N., Wisser, D., 2011. High-resolution mapping of the world's reservoirs and dams for sustainable river-flow management. Front. Ecol. Environ. 9, 494–502. https://doi.org/10.1890/100125

Lever, J., Krzywinski, M., Altman, N., 2017. Principal component analysis. Nat. Methods 14, 641–642. https://doi.org/10.1038/nmeth.4346

Li, X., Li, Y., He, J., Luo, X., 2016. Analysis of variation in runoff and impacts factors in the Yuanjiang-Red River Basin from 1956 to 2013. Resour. Sci. (in Chinese) 38, 1149–1159. https://doi.org/10.18402/resci.2016.06.14

Li, Y., He, D., Ye, C., 2008. Spatial and temporal variation of runoff of red river basin in Yunnan.

J. Geogr. Sci. 18, 308–318. https://doi.org/10.1007/s11442-008-0308-x

Li, Y., He, J., Li, X., 2016. Hydrological and meteorological droughts in the Red River Basin of Yunnan Province based on SPEI and SDI Indices (In Chinese). Prog. Geogr. 35, 758–767.

Liu, J., Duan, Z., Jiang, J., Zhu, A.-X., 2015. Evaluation of Three Satellite Precipitation Products TRMM 3B42, CMORPH, and PERSIANN over a Subtropical Watershed in China. Adv. Meteorol. 2015, 1–13. https://doi.org/10.1155/2015/151239

Lu, X.X., Oeurng, C., Le, T.P.Q., Thuy, D.T., 2015. Sediment budget as affected by construction of a sequence of dams in the lower Red River, Viet Nam. Geomorphology 248, 125–133. https://doi.org/10.1016/j.geomorph.2015.06.044

Ludwig, W., Probst, J.L., 1996. Predicting the oceanic input of organic carbon by continental erosion. Global Biogeochem. Cycles 10, 23–41. https://doi.org/10.1029/95GB02925

Luu, T.N.M., Garnier, J., Billen, G., Orange, D., Némery, J., Le, T.P.Q., Tran, H.T., Le, L.A., 2010. Hydrological regime and water budget of the Red River Delta (Northern Vietnam). J. Asian Earth Sci. 37, 219–228. https://doi.org/10.1016/j.jseaes.2009.08.004

Mai, V.T., van Keulen, H., Hessel, R., Ritsema, C., Roetter, R., Phien, T., 2013. Influence of paddy rice terraces on soil erosion of a small watershed in a hilly area of Northern Vietnam. Paddy Water Environ. https://doi.org/10.1007/s10333-012-0318-2

Manton, M.J., Della-Marta, P.M., Haylock, M.R., Hennessy, K.J., Nicholls, N., Chambers, L.E., Collins, D.A., Daw, G., Finet, A., Gunawan, D., Inape, K., Isobe, H., Kestin, T.S., Lefale, P., Leyu, C.H., Lwin, T., Maitrepierre, L., Ouprasitwong, N., Page, C.M., Pahalad, J., Plummer, N., Salinger, M.J., Suppiah, R., Tran, V.L., Trewin, B., Tibig, I., Yee, D., 2001. Trends in extreme daily rainfall and temperature in Southeast Asia and the South Pacific: 1961-1998. Int. J. Climatol. 21, 269–284. https://doi.org/10.1002/joc.610

Milliman, J.D., Meade, R.H., 1983. World-wide delivery of river sediment to the oceans. J. Geol. 91. https://doi.org/10.1086/628741

Milliman, J.D., Syvitski, J.P.M., 1992. Geomorphic/Tectonic Control of Sediment Discharge to the Ocean: The Importance of Small Mountainous Rivers. J. Geol. 100, 525–544. https://doi.org/10.1086/629606

Moriasi, D.N., Arnold, J.G., Van Liew, M.W., Bingner, R.L., Harmel, R.D., Veith, T.L., 2007. Model Evaluation Guidelines for Systematic Quantification of Accuracy in Watershed Simulations. Trans. ASABE 50, 885–900. https://doi.org/10.13031/2013.23153

Neitsch, S.., Arnold, J.., Kiniry, J.., Williams, J.., 2009. Soil and Water Assessment Tool Theoretical Documentation Version 2009. Texas Water Resour. Inst. https://doi.org/10.1016/j.scitotenv.2015.11.063

Nguyen, V.T., Orange, D., Laffly, D., Pham, V.C., 2012. Consequences of large hydropower dams on erosion budget within hilly agricultural catchments in Northern Vietnam by RUSLE modeling, in: International Conference Sediment Transport Modeling in Hydrological Watersheds and Rivers. Istanbul, Turkey, pp. 14–16.

Oeurng, C., Sauvage, S., Sánchez-Pérez, J.M., 2011. Assessment of hydrology, sediment and particulate organic carbon yield in a large agricultural catchment using the SWAT model. J. Hydrol. 401, 145–153. https://doi.org/10.1016/j.jhydrol.2011.02.017

Ouillon, S., 2018. Why and how do we study sediment transport? Focus on coastal zones and ongoing methods. Water (Switzerland) 10. https://doi.org/10.3390/w10040390

Peng, J., Chen, S., Dong, P., 2010. Temporal variation of sediment load in the Yellow River basin, China, and its impacts on the lower reaches and the river delta. CATENA 83, 135–147. https://doi.org/10.1016/j.catena.2010.08.006

Phan, D.B., Wu, C.C., Hsieh, S.C., 2010. Land Use Change Effects on Discharge and Sediment Yield of Song Cau Catchment in Northern Vietnam. J. Environ. Sci. Eng. 5, 92–101.

Podwojewski, P., Orange, D., Jouquet, P., Valentin, C., Nguyen, V.T., Janeau, J.L., Tran, D.T., 2008. Land-use impacts on surface runoff and soil detachment within agricultural sloping lands in Northern Vietnam. Catena 74, 109–118. https://doi.org/10.1016/j.catena.2008.03.013

Ranzi, R., Le, T.H., Rulli, M.C., 2012. A RUSLE approach to model suspended sediment load in the Lo river (Vietnam): Effects of reservoirs and land use changes. J. Hydrol. 422–423, 17–29. https://doi.org/10.1016/j.jhydrol.2011.12.009

Ren, J., He, D., Fu, K., Li, Y., 2007. Sediment variation in the Yuanjiang (the Red River Basin) driven by climate change and human activities (in Chinese). Chinese Sci. Bull. 52, 142–147. https://doi.org/https://doi.org/10.1360/csb2007-52-zkII-142

Ringnér, M., 2008. What is principal component analysis? Nat. Biotechnol. 26, 303–304. https://doi.org/10.1038/nbt0308-303

Simons, G., Bastiaanssen, W., Ngô, L., Hain, C., Anderson, M., Senay, G., 2016. Integrating Global Satellite-Derived Data Products as a Pre-Analysis for Hydrological Modelling Studies: A Case Study for the Red River Basin. Remote Sens. 8, 279. https://doi.org/10.3390/rs8040279

Syvitski, J.P., Morehead, M.D., Bahr, D.B., Mulder, T., 2000. Estimating fluvial sediment transport: The rating parameters. Water Resour. Res. 36, 2747–2760. https://doi.org/10.1029/2000WR900133

Syvitski, J.P.M., Peckham, S.D., Hilberman, R., Mulder, T., 2003. Predicting the terrestrial flux of sediment to the global ocean: A planetary perspective. Sediment. Geol. 162, 5–24. https://doi.org/10.1016/S0037-0738(03)00232-X

Syvitski, J.P.M., Vorosmarty, C.J., Kettner, A.J., Green, P., 2005. Impact of Humans on the Flux of Terrestrial Sediment to the Global Coastal Ocean. Science. 308, 376–380. https://doi.org/10.1126/science.1109454

the World Commission on Dams, 2000. Dams and Development: A New Framework for Decision-Making.

Tuan, V.D., Hilger, T., MacDonald, L., Clemens, G., Shiraishi, E., Vien, T.D., Stahr, K., Cadisch, G., 2014. Mitigation potential of soil conservation in maize cropping on steep slopes. F. Crop. Res. 156, 91–102. https://doi.org/10.1016/j.fcr.2013.11.002

Valentin, C., Agus, F., Alamban, R., Boosaner, A., Bricquet, J.P., Chaplot, V., de Guzman, T., de Rouw, A., Janeau, J.L., Orange, D., Phachomphonh, K., Do Duy Phai, Podwojewski, P., Ribolzi, O., Silvera, N., Subagyono, K., Thiébaux, J.P., Tran Duc Toan, Vadari, T., 2008. Runoff and sediment losses from 27 upland catchments in Southeast Asia: Impact of rapid land use changes and conservation practices. Agric. Ecosyst. Environ. 128, 225–238. https://doi.org/10.1016/j.agee.2008.06.004

Vigiak, O., Malagó, A., Bouraoui, F., Vanmaercke, M., Poesen, J., 2015. Adapting SWAT hillslope erosion model to predict sediment concentrations and yields in large Basins. Sci. Total Environ. https://doi.org/10.1016/j.scitotenv.2015.08.095

Vinh, V.D., Ouillon, S., Thanh, T.D., Chu, L. V., 2014. Impact of the Hoa Binh dam (Vietnam) on water and sediment budgets in the Red River basin and delta. Hydrol. Earth Syst. Sci. 18, 3987–4005. https://doi.org/10.5194/hess-18-3987-2014

Vörösmarty, C.J., Meybeck, M., Fekete, B., Sharma, K., Green, P., Syvitski, J.P.M., 2003. Anthropogenic sediment retention: Major global impact from registered river impoundments. Glob. Planet. Change 39, 169–190. https://doi.org/10.1016/S0921-8181(03)00023-7

Walling, D.E., Fang, D., 2003. Recent trends in the suspended sediment loads of the world's rivers. Glob. Planet. Change 39, 111–126. https://doi.org/10.1016/S0921-8181(03)00020-1

Wang, H., Wu, X., Bi, N., Li, S., Yuan, P., Wang, A., Syvitski, J.P.M., Saito, Y., Yang, Z., Liu, S., Nittrouer, J., 2017. Impacts of the dam-orientated water-sediment regulation scheme on the lower reaches and delta of the Yellow River (Huanghe): A review. Glob. Planet. Change 157, 93–113. https://doi.org/10.1016/j.gloplacha.2017.08.005

Wei, X., Sauvage, S., Le, T.P.Q., Ouillon, S., Orange, D., Vinh, V.D., Sanchez-Perez, J.-M., 2019. A Modeling Approach to Diagnose the Impacts of Global Changes on Discharge and Suspended Sediment Concentration within the Red River Basin. Water 11, 958. https://doi.org/10.3390/w11050958

Williams, J.R., 1975. Sediment Routing for Agricultural Watersheds. JAWRA J. Am. Water Resour. Assoc. 11, 965–974. https://doi.org/10.1111/j.1752-1688.1975.tb01817.x

Wold, S., Esbensen, K., Geladi, P., 1987. Principal component analysis. Chemom. Intell. Lab. Syst. 2, 37–52. https://doi.org/10.1016/0169-7439(87)80084-9

Xie, S., 2002. The Hydrological Characteristics of the Red River Basin. Hydrol. (in Chinese) 22, 57–63. https://doi.org/10.3969/j.issn.1000-0852.2002.04.017

Xu, Z.X., Pang, J.P., Liu, C.M., Li, J.Y., 2009. Assessment of runoff and sediment yield in the Miyun Reservoir catchment by using SWAT model. Hydrol. Process. 23, 3619–3630. https://doi.org/10.1002/hyp.7475

Yang, D., Kanae, S., Oki, T., Koike, T., Musiake, K., 2003. Global potential soil erosion with reference to land use and climate changes. Hydrol. Process. 17, 2913–2928. https://doi.org/10.1002/hyp.1441

Zarfl, C., Lumsdon, A.E., Berlekamp, J., Tydecks, L., Tockner, K., 2015. A global boom in hydropower dam construction. Aquat. Sci. 77, 161–170. https://doi.org/10.1007/s00027-014-0377-0

Zhang, W., Zhao, Z., Tan, S., Li, Y., Wang, A., 2017. Study on the soil erosion in the Yuanjiang - Honghe boundary river areas (in Chinese). Geol. Surv. China 4, 64–69. https://doi.org/10.19388 /j.zgdzdc.2017. 03.10

Zimmerman, J.B., Mihelcic, J.R., Smith, J., 2008. Global stressors on water quality and quantity, Environmental Science and Technology. https://doi.org/10.1021/es0871457

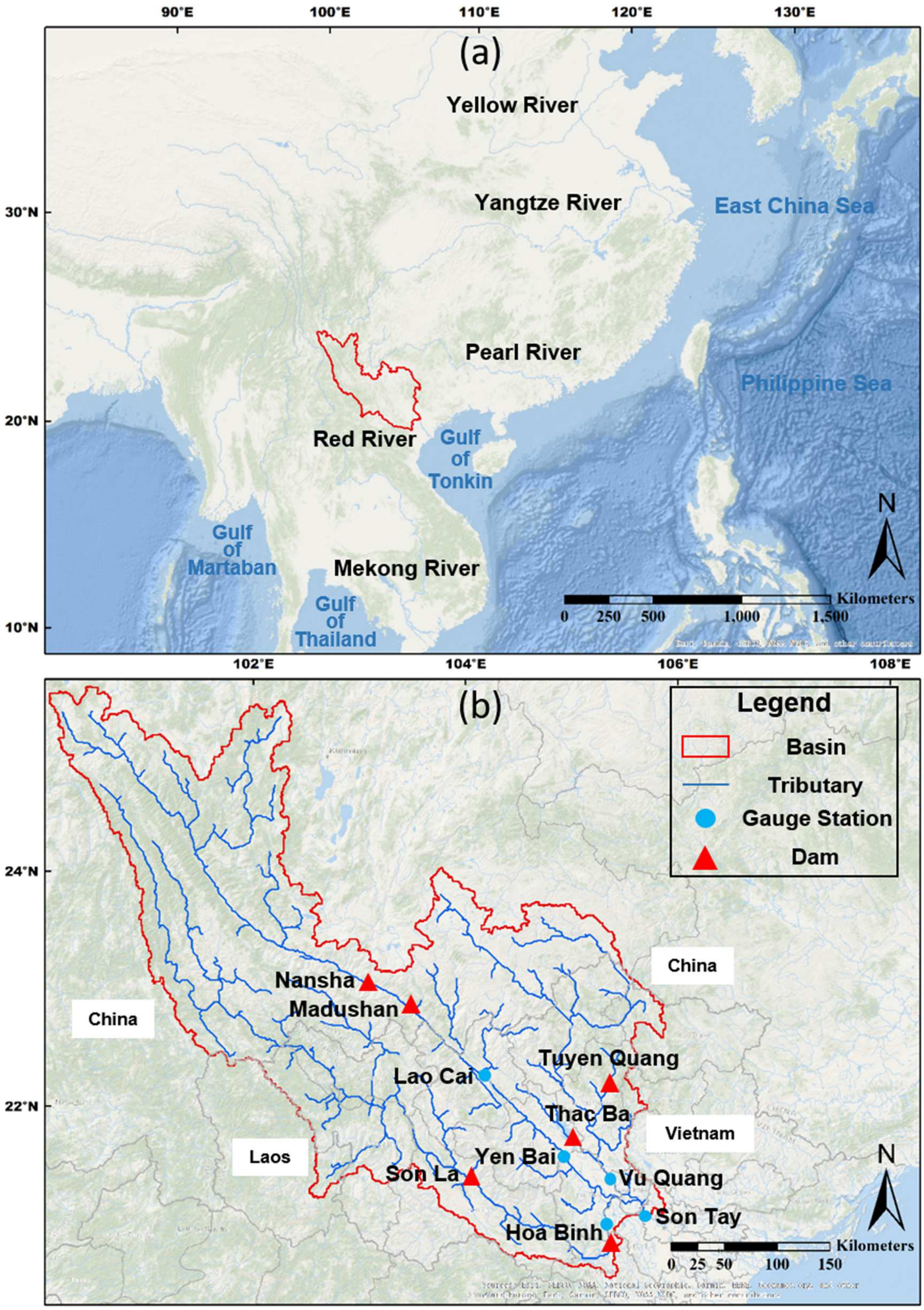

Figure 1. (a) The geographical location of the Red River basin in Southeast Asia; (b) locations of the dams (red triangle) and the hydrological gauge stations (blue point) in the Red River basin. Base maps sources were obtained from ArcGIS desktop.

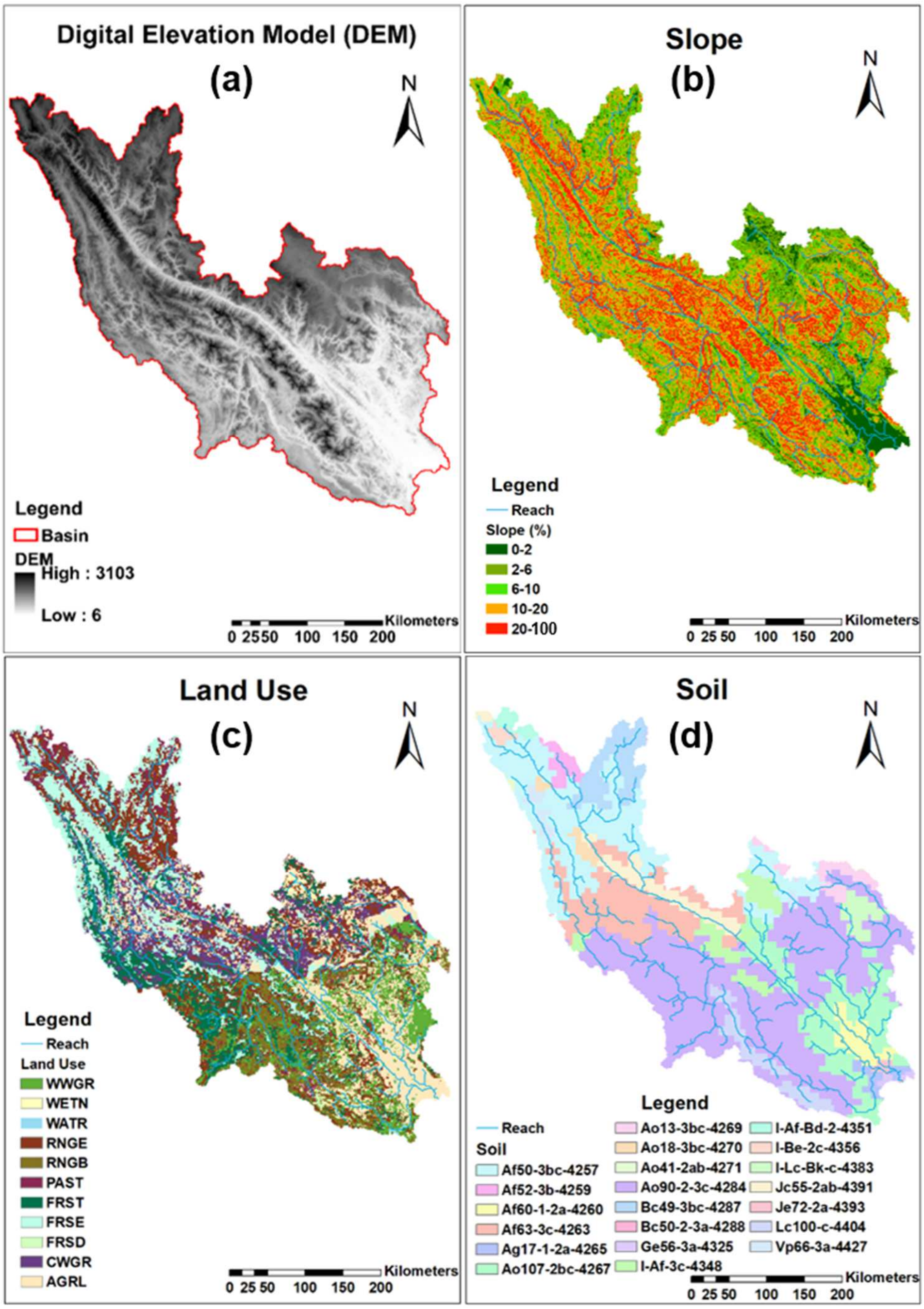

Figure 2: (a) digital elevation model (gray shades); (b) slope classes: slopes were divided into 5 classes by SWAT based on the (DEM); (c) land use map; (d) soil types. Data sources are presented in the supplementary material (Table S-1), and the legends of land use and soil are detailed in the supplementary material (Tables S-2 and S-3).

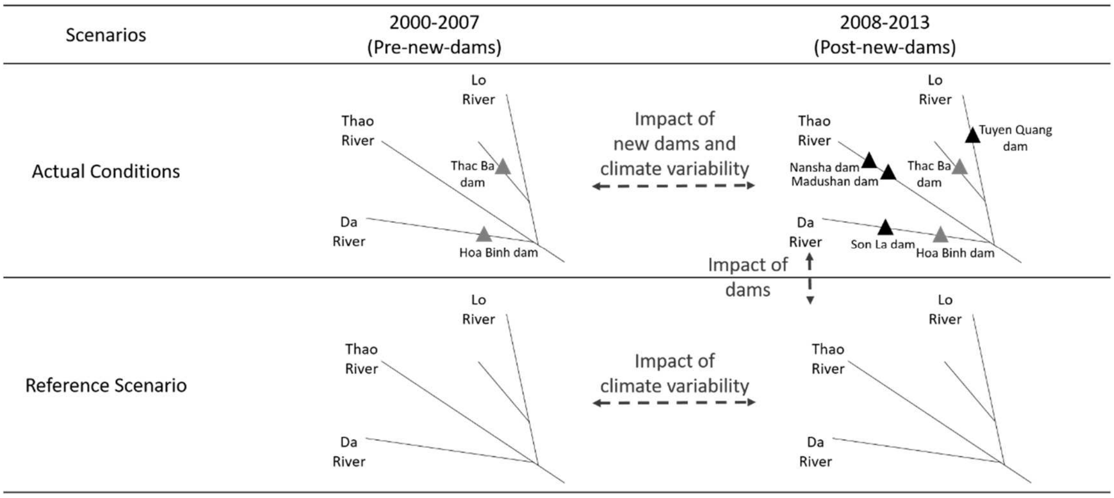

Figure 3. Scenarios setting: actual conditions and reference scenario. Gray triangles are the old dams built before 2000 and black triangles are the new dams built after 2007.

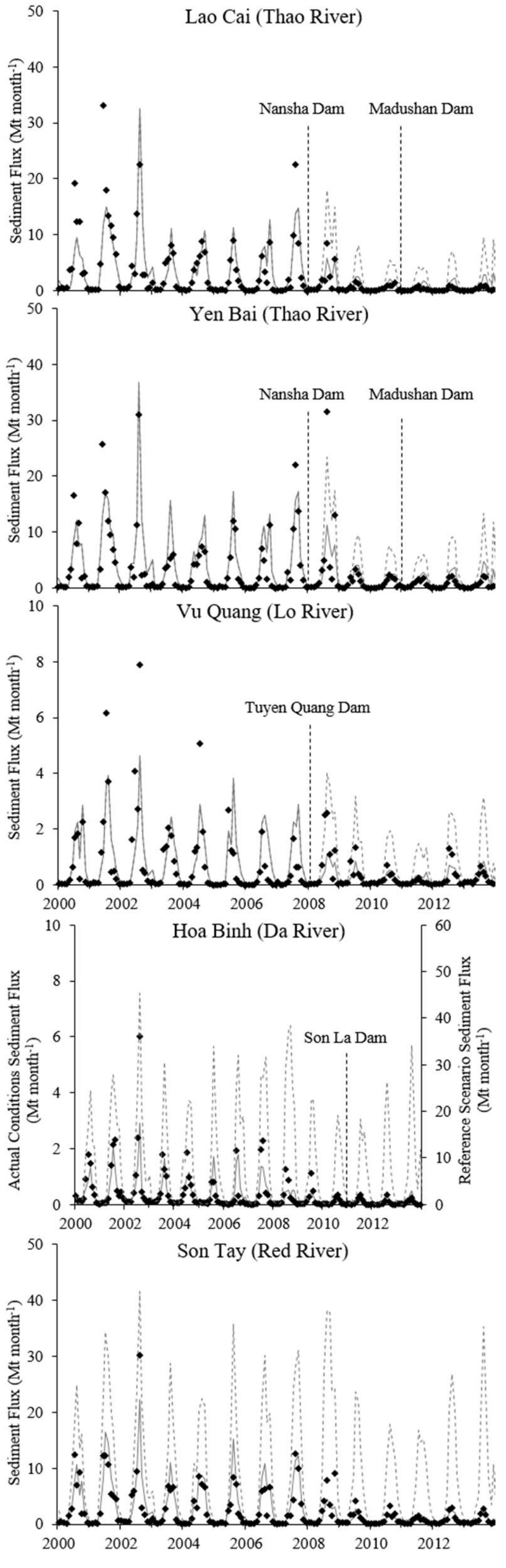

Figure 4. Observed (black dot) and simulated (gray solid line) monthly sediment flux, and simulated sediment flux of reference scenario (without dams, gray dash line) at five stations from 2000 to 2013.

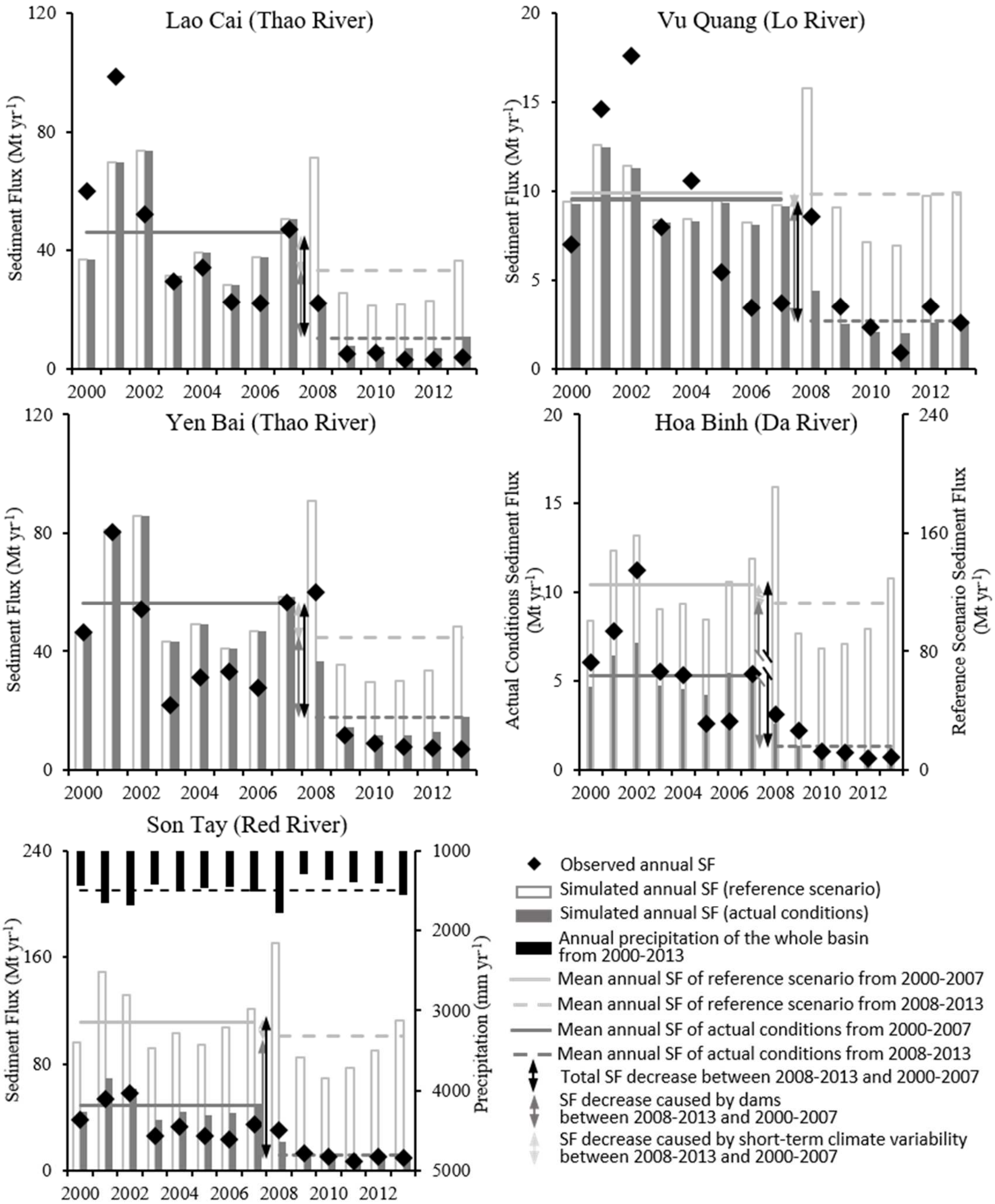

Figure 5. Annual sediment flux (SF) variation from 2000-2013 at 5 gauge stations, and the mean annual SF of pre-new-dams (2000-2007) and post-new-dams (2008-2013). The annual precipitation variation of the whole basin from 2000-2013.

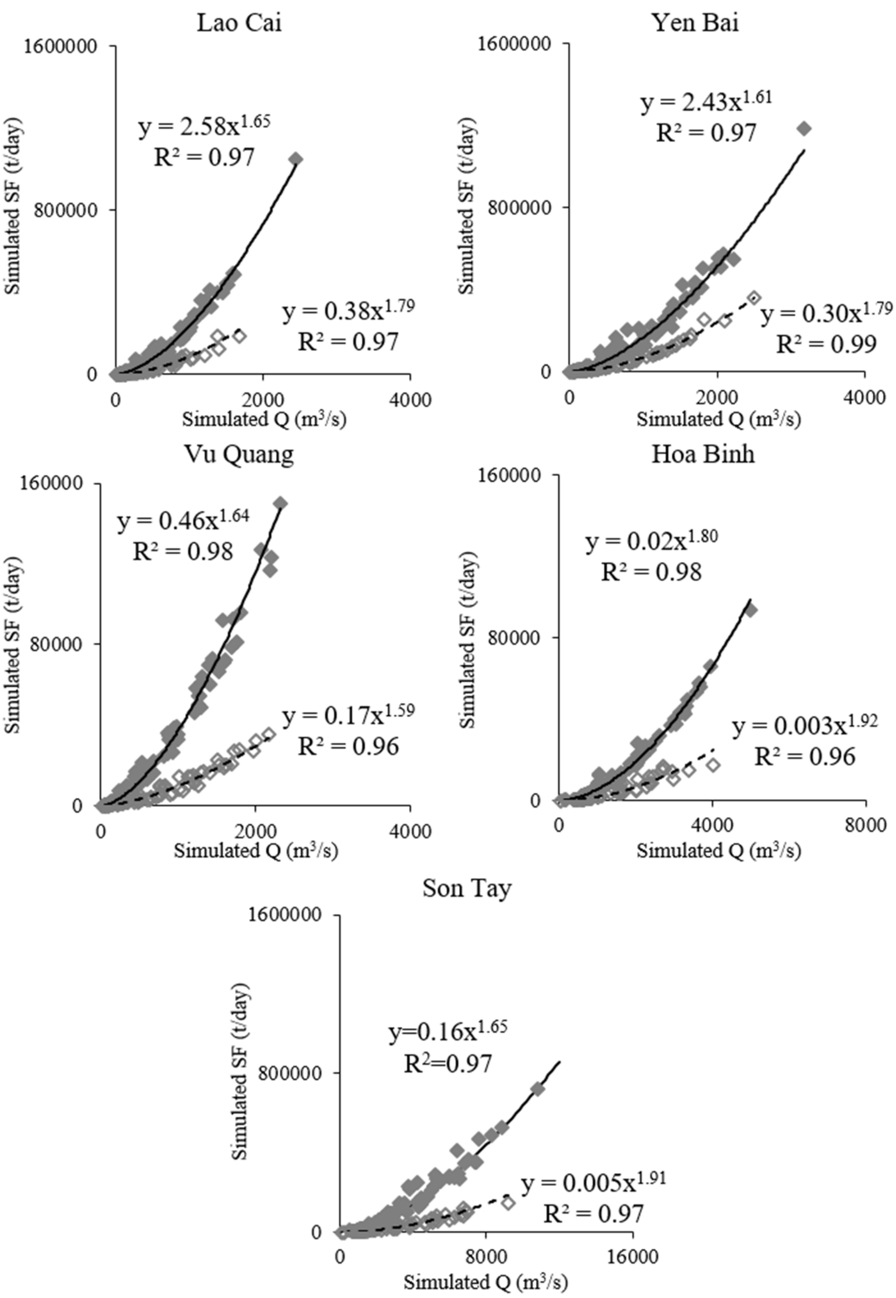

Figure 6. Correlation and relations between simulated monthly mean discharge (Q) and simulated monthly mean sediment fluxes (SF) at 5 stations in the simulation under actual conditions. Gray solid squares are of the period 2000-2007; gray hollow squares are of the period 2008-2013. Black solid and dash lines are the fitting curves of the period 2000-2007 and 2008-2013, respectively.

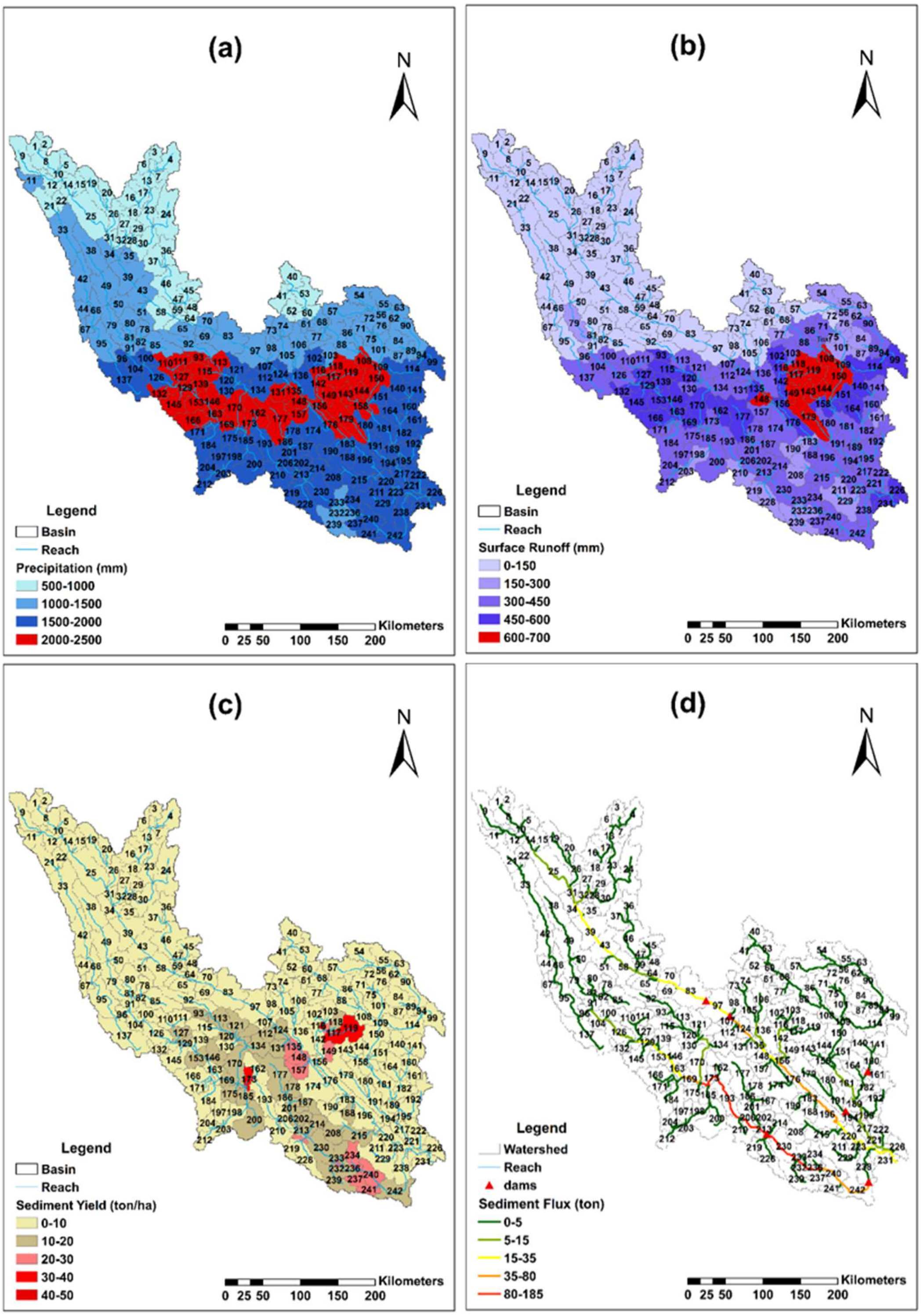

Figure 7. Mean annual value of (a) Precipitation distribution (mm yr^{-1}), (b) Surface Runoff (mm yr^{-1}), (c) Soil Erosion (ton ha^{-1} yr^{-1}), (d) In-stream Sediment Flux (ton yr^{-1}) within 242 sub-basins, derived from the actual conditions simulation over the period 2000-2013.

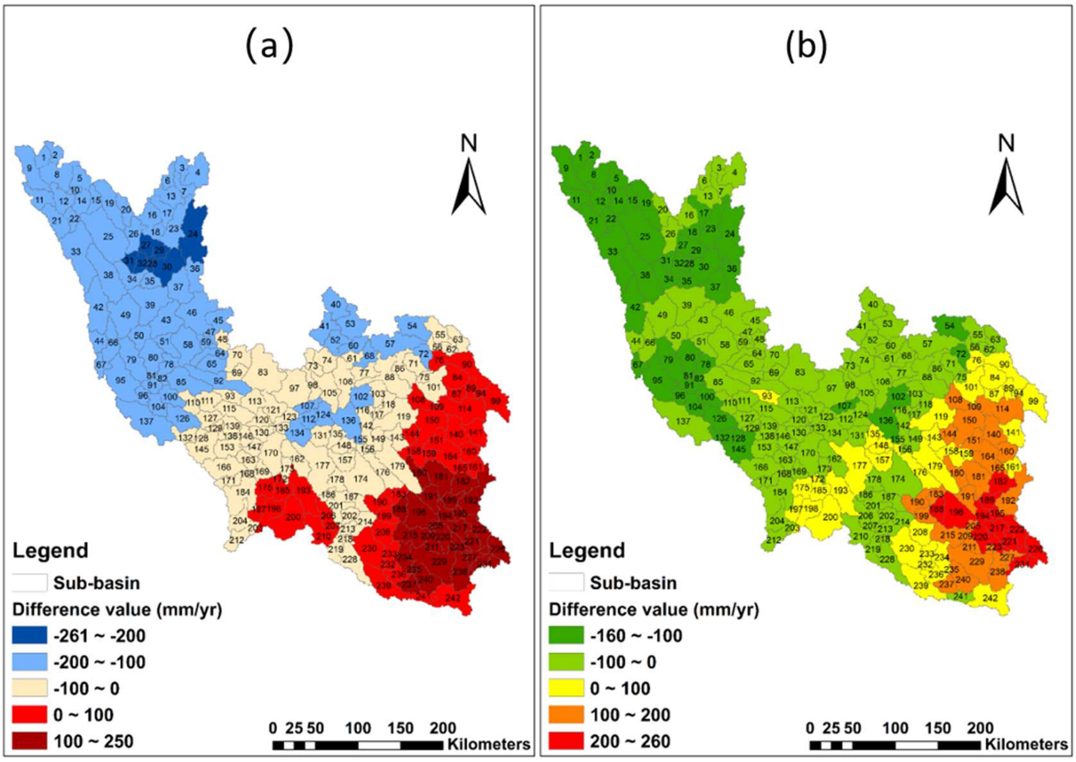

Figure 8. The differences in annual rainfall (a) and annual water availability (b) between 2008-2013 and 2000-2007.

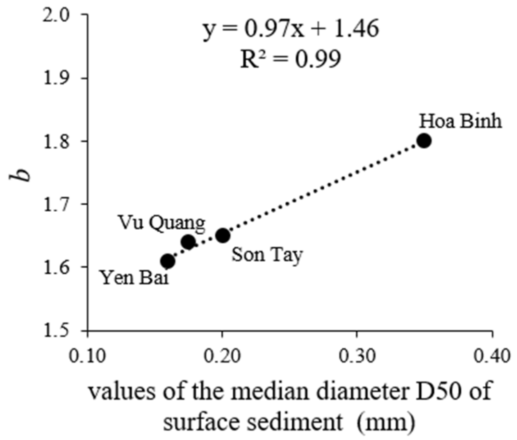

Figure 9. Relationship between the parameter *b* and the values of the median diameter D50 of surface sediment.

Table 1 Basic characteristics of the main dams in the Red River basin (Le et al., 2017; Wei et al., 2019)

Dam	Basin	Construction began	Impoundment	Capacity (km^3)
Nansha	Thao	Feb-06	Nov-07	0.26
Madushan	Thao	Dec-08	Dec-10	0.55
Thac Ba	Lo	1965	1971	2.90
Tuyen Quang	Lo	Dec-02	Mar-08	2.24
Hoa Binh	Da	1980	1989	9.50
Son La	Da	Dec-05	Dec-10	9.26

Table 2 Annual mean and seasonal variation of observed discharge (Q) and suspended sediment concentration (SSC) for 2000-2013 at 5 gauge stations.

Gauge Station (Basin)	Drained Area (km^2)	Q (m^3/s)		SSC (mg/L)	
		Annual Mean	Seasonal Variation	Annual Mean	Seasonal Variation
Lao Cai (Thao)	41600	520	210-1123	800	181-1963
Yen Bai (Thao)	58500	652	218-1577	724	163-1758
Vu Quang (Lo)	30370	891	408-2138	111	22-272
Hoa Binh (Da)	52780	1638	692-3997	42	18-107
Son Tay (Red)	137230	3122	1231-7152	164	55-367

Table 3 Evaluation statistics of sediment flux (SF) on different time scales for each station from 2000 to 2013

Sediment Flux	Statistics	Stations				
		Lao Cai	Yen Bai	Vu Quang	Hoa Binh	Son Tay
Monthly Scale	NSE	0.67	0.66	0.62	0.72	0.71
	R^2	0.68	0.69	0.62	0.75	0.79
	PBIAS	-1.8	-8.7	-0.9	4.6	-24.5
Annual Scale	NSE	0.78	0.60	0.55	0.73	0.54
	R^2	0.78	0.73	0.55	0.77	0.86
	PBIAS	-5.2	-22.6	-0.8	8.6	-24.7

Table 4 Seasonal variation of sediment fluxes and mean monthly sediment fluxes for flood and dry seasons at five gauge stations

Gauge Stations	**Drained Area** (km^2)	**Seasonal Variations** ($Mt\ month^{-1}$)	**Flood Season (May-Oct)**		**Dry Season (Nov-Apr)**	
			Flux ($Mt\ month^{-1}$)	Specific Yield ($t\ km^{-2}\ month^{-1}$)	Flux ($Mt\ month^{-1}$)	Specific Yield ($t\ km^{-2}\ month^{-1}$)
Lao Cai	41600	0.0005-34.4	4.5	108.2	0.7	16.8
Yen Bai	48500	0.0007-39.6	5.8	119.6	0.8	16.5
Vu Quang	30370	0.0006-4.7	1.1	36.2	0.1	3.3
Hoa Binh	52780	0.0003-3.0	0.5	9.5	0.1	1.9
Son Tay	137230	0.0014-25.2	4.4	32.1	0.5	3.6

Table 5 Simulated sediment flux (Mt yr^{-1}) of reference scenario (without dams) and actual conditions (over the whole study period, 2000-2007 period and 2008-2013 period) compared with other studies and in-situ data; values of trapped sediment (calculated as the difference between average values over 2008-2013 in the reference scenario and actual simulations); impacts of short-term climate variability and dams.

Station	**1960-1972**	**1960-1979**	**1960-1970**	**2000-2013**			**2000-2007**			**2008-2013**				**Impact**		
(River)	(Lu et al., 2015)	(Vinh et al., 2014)	(Dang et al., 2010)	Observed	AC†	RS‡	Observed	AC†	RS‡	Observed	AC†	RS‡	Trapped sediment	Total	Short-term climate variability	Dams
Lao Cai (Thao)	-	-	-	29.2	30.7	40.5	45.7	46.0	46.0	7.1	10.3	33.3	23.0	-78%	-28%	-50%
Yen Bai (Thao)	44.8	43.4	-	32.5	39.8	51.4	43.9	56.5	56.5	17.2	17.6	44.6	27.0	-69%	-21%	-48%
Vu Quang (Lo)	10.1	9.2	-	6.6	6.6	9.7	8.8	9.6	9.5	3.6	2.7	9.8	7.1	-72%	2%	-74%
Hoa Binh (Da)	71.8	65.0	-	4.0	3.6	119.5	5.8	5.3	124.9	1.5	1.3	112.3	111.0	-99%	-10%	-89%
Son Tay (Red)	120.8	119.3	111.6	26.5	33.0	106.9	36.5	49.1	111.6	13.2	11.6	100.6	89.0	-90%	-10%	-80%

AC†: Actual Conditions

RS‡: Reference Scenario (without dams)

Table 6 The principal component (PC) loading

Factor	Eigenvectors (percentage of variances %)		
	PC1 (41.6%)	**PC2 (25.9%)**	**PC3 (10.8%)**
Soil Erosion (SE)†	0.177	0.399	0.163
Precipitation (P)‡	0.430	0.244	0.101
Water Yield (WY)‡	0.416	0.262	0.095
Surface Runoff (SR)‡	0.446	0.184	-0.033
Slope†	-0.067	0.491	0.125
Clay%†	-0.389	0.117	0.277
Silt%†	0.019	0.243	-0.877
Sand%†	0.346	-0.280	0.256
USLE_P†	-0.246	0.414	0.158
USLE_K†	-0.275	0.340	0.050

†: the simulation from the model

‡: the observation and input data

Notes: underlined values correspond to the first three highest factor loadings in the PC.

A modelling-based assessment of suspended sediment transport related to new damming in the Red River basin from 2000-2013

Xi Wei[1*], Sabine Sauvage[1**], Sylvain Ouillon[2,3], Thi Phuong Quynh Le[4], Didier Orange[5], Marine Herrmann[2,3], José-Miguel Sanchez-Perez[1]